Schweizerische Eidgenossenschaft
Confédération suisse
Confederazione Svizzera
Confederaziun svizra

Federal Department of the Environment, Transport, Energy and Communications DETEC

**Swiss Federal Office of Energy SFOE**
Energy Research and Cleantech Division

# REEL Demo – Romande Energie ELectric network in local balance Demonstrator

## Deliverable: 5 Overall Performance of the implemented solutions with guidelines for subsequent implementation

## Demo site: Rolle

Developed by
Luise MIDDELHAUVE (EPFL-IPESE)
with the Collaboration of
Luc GIRARDIN (EPFL-IPESE)

[Sion, 27.03.2021]

# Contents

Open Government Data

# Nomenclature

**ACRONYMS**

| | |
|---|---|
| BES | Building energy system |
| CAPEX | Capital expenses |
| CPT | Carbon Payback Time |
| DES | District energy systems |
| DHW | Domestic hot water |
| ETES | Electro-thermal energy storage |
| GHG | Greenhouse gas |
| GIS | Geographic information systems |
| GM | Grid multiple |
| GWP | Global warming potential |
| HP | Heat pump |
| HVAC | Heating, ventilation and air conditioning |
| IPCC | Intergovernmental Panel on Climate Change |
| KPI | Key performance indicator |
| LDC | Load duration curve |
| MAE | Mean average error |
| MAPE | Mean average percentage error |
| MILP | Mixed-integer linear programming |
| MOO | Multi-objective optimization |
| NG | Natural gas |
| NLP | Non linear programming |
| OCC | Occupancy |
| OGD | |
| OPEX | Operational expenses |
| P2G | Power to gas |
| PHS | Pumped hydro storage |
| PV | Photovoltaic |
| PVP | Photovoltaic penetration |
| RMSD | Root mean square deviation |
| SC | Self-consumption |
| SH | Space heating |
| SS | Self-sufficiency |
| TOTEX | Total expenses |

**SETS**

| | | |
|---|---|---|
| A | azimuth | $\alpha$ |
| B | building | b |
| I | interval | i |
| K | temperature interval | c |
| P | patch | pt |
| P | period | p |
| R | replacement | r |
| T | tilt | $\gamma$ |
| T | timestep | t |
| U | utility | u |

**SYMBOLS**

| | | |
|---|---|---|
| $\alpha$ | azimuth angle | $^\circ$ |
| $\beta$ | design limiting angle | $^\circ$ |
| $\boldsymbol{C}$ | cost | CHF |
| $\boldsymbol{E}$ | electricity | kW(h) |
| $\boldsymbol{f}$ | sizing variable | $\diamond$ |
| $\boldsymbol{G}$ | global warming potential | $kg_{CO2,eq}$ |
| $\boldsymbol{H}$ | natural gas or fresh water | kW(h) |
| $\boldsymbol{Q}$ | thermal energy | kWh |
| $\boldsymbol{R}$ | residual heat | kWh |
| $\boldsymbol{T}$ | temperature | K |
| $\boldsymbol{y}$ | decision variable, binary | [-] |
| $\epsilon$ | elevation angle | $^\circ$ |
| $\eta$ | efficiency | - |
| $\gamma$ | tilt angle | $^\circ$ |

| | | |
|---|---|---|
| $\Phi$ | specific heat gain | kW/ $m^2$ |
| $\rho$ | density | kg/$m^3$ |
| $A$ | area | $m^2$ |
| $b$ | baremodule | - |
| $C$ | heat capacity coefficient | kW/$m^2$K |
| $c$ | energy tariff | CHF/kWh |
| $c_p$ | specific heat capacity | kJ(/ (kg K) |
| $d$ | distance | m |
| $d_p$ | frequency of periods per year | d/yr |
| $d_t$ | frequency of timesteps per period | h/d |
| $F$ | bound unit size | $\diamond$ |
| $f^s$ | solar factor | - |
| $f^u$ | usage factor | - |
| $f_{b,r}$ | spatial fraction of room in building | - |
| $g$ | g - value | - |
| $g$ | global warming potential | $kg_{CO2,eq}$ /kWh |
| $h$ | height | m |
| $i$ | interest rate | - |
| $i^{c1}$ | fixed investment cost | CHF |
| $i^{c2}$ | continuous investment cost | CHF/ $\diamond$ |
| $i^{g1}$ | fixed impact factor | $kg_{CO2,eq}$ |
| $i^{g2}$ | continuous impact factor | $kg_{CO2,eq}$/ $\diamond$ |
| $irr$ | irradiation density | kWh/$m^2$ |
| $l$ | lifetime | yr |
| $n$ | number/ quantity | - |
| $n$ | project horizon | yr |
| $Q$ | thermal energy | kW |
| $s$ | shading factor | - |
| $T$ | temperature | K |
| $U$ | heat transfer coefficient | kW/$m^2$K |
| $V$ | volume | $m^3$ |
| $x, y, z$ | coordinates | - |

**SUBSCRIPTS/SUPERSCRIPTS**

| | |
|---|---|
| $+$ | supply |
| $-$ | demand |
| $A$ | appliance |
| $B$ | building |
| $bes$ | building energy system |
| $cap$ | capital |
| $cw$ | cold water |
| $dhw$ | domestic hot water |
| $el$ | electricity |
| $era$ | energy reference area |
| $ext$ | external |
| $g$ | glass |
| $gain$ | heat gain |
| $gr$ | grid |
| $int$ | internal |
| $inv$ | investment |
| $irr$ | irradiation |
| $L$ | light |
| $lca$ | life cycle assessment |
| $max$ | maximum |
| $min$ | minimum |
| $net$ | netto |
| $ng$ | natural Gas |
| $op$ | operation |
| $P$ | people |
| $pv$ | photovoltaic panel |
| $r$ | return |
| $ref$ | reference |
| $rep$ | replacement |
| $s$ | supply |
| $SH$ | space heating |
| $TR$ | transformer |

# Executive summary

The foreseen important increase of the penetration of distributed renewable energies technologies into the electricity distribution grid is expected to lead to some major challenges. On the one hand, a large and synchronous production could lead in certain time periods to a surplus of production, exceeding the consumption needs and resulting in a zero or negative market value of electricity that may deter any incentive to further invest in certain sources of renewable energy. This production surplus is also expected to lead to grid congestion, transformer overloading and overvoltage situations that will critically affect grid operation. Yet, if the renewable energies technologies, storage devices, and electrified loads are exploited through coordinated control mechanisms they could also offer new opportunities for stakeholders.

The JA-RED partners have therefore developed methods to evaluate the long-term implementation of decentralized solutions that could be massively deployed to decarbonize and denuclearize the Swiss energy mix, while providing economic opportunities for all stakeholders.

This report takes a deeper look at the implemented decentralized energy solutions integrating heat pumps, heat storage, batteries and solar panels considering shading effect, not only on roofs, but also on facades of the district which indeed host 70% of the available PV area and near half of the generation potential. Achieving self-sufficiency at district scale is challenging: it can be achieved by covering approximately 42% to 100% of the available surface when the round trip efficiency decreases from 100% to 50%.

The results underlined the importance of storage for achieving self-sufficiency: even with 100% round trip efficiency for the storage, very large capacities are required. Moreover, the grid revenues generated by the difference between retail and feed-in prices are not sufficient to pay for the storage required to make the district self-sufficient, suggesting that public funding would be crucial for supporting these developments. This arise with relatively low installed PV capacity ($A_{PV}/A_{SRE} = 0.2$), when storage starts to be seasonal rather than daily. However, energy demand reduction through renovation would allow to reach self-sufficiency with half of the PV and storage capacity required for the actual building stock, and the deployment of additional long-term storage capacity could be implemented together with the development of the next 5$^{th}$ generation of district heating and cooling systems [1], realizing sector coupling with power to gas (P2G) and electro-thermal energy storage (ETES).

# 1. Description of deliverable and goal

The present deliverable leverage on the publication in submission:

**Luise Middelhauve, Luc Girardin, Francesco Baldi, François Maréchal, "Potential of Photovoltaic Panels on Building's envelope for Decentralized District Energy Systems, IPESE-EPFL, 2021**.

It is the last of a serie of joint activity (JA-RED) studies for the implementation of future decentralized renewable district energy systems using the RE site as a demonstrator.

Previous studies [2], have shown that (i) more than 90% of the solar potential on roof of buildings is still untapped, while (ii) district heating and cooling network is yet to be developed with (iii) a strategic vision of the future role of gas and biogas. A building to district and district to grid approach has therefore been implemented [3] allowing to generate and evaluate the impact on the grid of a wide range of optimal energy transition scenarios [4].

The present work takes a deeper look at the implementation of decentralized energy solutions integrating heat pumps, heat storages, batteries and solar panels considering shading effect, not only on roofs, but also on facades of the district. This cover in particular the study of strategies to maximize long-term system deployment and integration while minimizing the grid impact and providing economic opportunities for all stakeholders.

## 1.1. Novelty of the proposed solutions compared to the state-of-art

The comparative analysis of the state of the art of research in the role of facades in urban energy systems shows that most available studies only consider facade PV systems on their own, and do not explore the importance of their interaction with the rest of the building energy system building energy system (BES). These studies are usually conducted from the perspective of urban planners and architects, and are aimed at assessing the solar potential on the complete envelope to find best concept and designs of buildings.

Papers focusing on the design the energy system of buildings includes irradiation models to assess the solar contribution to the heating and cooling demand and model the contribution of solar panels (both thermal and PV) to BES. [5, 6]. However, in most cases, these works rely on the use of global irradiation to model the incoming solar radiation. This corresponds to assuming horizontal panels [7], a simplification that was shown to generate a relevant error (over-estimation or under-estimation, depending on the case) in the calculation of how much energy is generated by solar systems [8].

In the proposed building to district model, each building is a prosumer contributing to the overall energy balance of the district where solar generation profiles are impacted by shading effects. This fills a gap in the previous methods and tools by integrating oriented photovoltaic (PV) modules on both roofs and facades with the optimal design and operation of conversion and storage technologies.

## 1.2. Research question

The foreseen important increase of the penetration of distributed renewable energies technologies into the electricity distribution grid is expected to lead to some major challenges. On the one hand, a large and synchronous production could lead in certain time periods to a surplus of production, exceeding the consumption needs and resulting in a zero or negative market value of electricity that may deter any incentive to further invest in certain sources of renewable energy. This production surplus is also expected to lead to grid congestion, transformer overloading and overvoltage situations that will critically affect grid operation. Yet, if the renewable energies technologies, storage devices, and electrified loads are exploited through coordinated control mechanisms they could also offer new opportunities for stakeholders. Thus, the partners have aimed at tackling the following research questions:

- can decentralized energy transition solutions be massively deployed to decarbonize the Swiss eneergy mix ?
- what are the optimal strategies for the long-term implementation of decentralized solutions minimizing grid impact and providing economic opportunities for all stakeholders ?
- what are the driving forces and bottlenecks for this long term deployment, for prosumers and network operators.

# 2. Achievement of Deliverable

This work has closed a gap in the previous methods and tools by integrating oriented PV modules on both roofs and facades in the optimal design and operation of conversion and storage technologies. The proposed approach provides strategies to maximize long-term deployment and integration while minimizing the grid impact and providing economic opportunities for all stakeholders.

Existing methods and tools have been improved, allowing the simultaneous integration oriented PV modules on both roofs and facades with the optimal design and operation of conversion and storage technologies. More precisely, the model allows to:

- integrate shading effect and orientation of PV in the optimization of energy systems;
- Investigate the choice on the economic and environmental rationale for installing PV panels on facades and, if so, on which ones.
- evaluate the economical benefice of large scale PV implementation in roof and facade of urban districts, giving the amount of square meter needed to reach self-sufficient and carbon-neutrality at district scale;
- estimate the amount of electricity generated from the district that, from the perspective of the electricity grid, needs to be distributed or stored, and the related costs.

## 2.1. Date

This deliverable is handed in March 2021.

## 2.2. Demonstration of the Deliverable

The proposed approach has been demonstrated on a reference district of the RE demonstrator including 31 buildings connected to a measured transformer.

# 3. Impact

Our objective within the REel demo project has been to develop urban energy planning methods to make recommendations for the integration of renewable energy in complex energy system. In line with the Energy Strategy 2050 and target of the article 89 ”Energy policy” of the Swiss constitution, the study contribute to the consortium's overall impact by the development of methods and tools demonstrating the conditions under which the implementation of decentralized urban energy system is economically feasible

Finally, a great part of the work presented in this report has been valued in an open access publication ”Potential of Photovoltaic Panels on Facades for Decentralized District Energy Systems”.

# 4. Introduction

Political authorities and other stakeholders in the energy value chain have the responsibility to implement energy transition pathways by increasing decentralized renewable energy generation. As a main stakeholder, authorities often lack the appropriate tools to frame and encourage the transition, and monitor the impact of energy transition policies. Network operators as well need appropriate frameworks and guidelines to implement the transition with a business perspective.

The electrification of the buildings stock, switching from fossil fuel to heating, ventilation and air conditioning (HVAC) systems, lower local pollutant emissions and increase the energy system efficiency by harvesting local renewable energy sources [1, 9]. Roofs constitute the most obvious solution for the integration of PV generation in buildings [10]. Actually, more than 90% of the solar potential on the top of roofs are still unexploited and little used for other purposes, while horizontal and low-tilted surfaces generally have the highest yields with respect to the surface occupied by the panels. With the recent decrease in PV systems' investment costs, rooftop PV is a proven, cost-convenient choice in many parts of the world, even in absence of subsidies [11]

When looking at urban environments, roofs constitute the most obvious solution for the implementation of PV generation in the system. Roofs are surfaces that are generally little used for other purposes, and horizontal and low-tilted surfaces generally have the highest yields with respect to the surface occupied by the panels. With the recent decrease in PV systems' investment costs, rooftop PV is a proven, cost-convenient choice in many parts of the world, even in absence of subsidies [11].

In urban environments, however, the limited available space for including locally generated renewable energy compared to the energy demand makes up for an additional challenge towards a complete decarbonization of the energy system. As a result of this challenge, together with the low cost of PV modules, research in recent years also focused on the role of facades in urban context.

Initial feasibility studies focused on a general estimation of the potential from PV facades, introducing the concept of vertically oriented surfaces [12]. These early studies, however, did not consider PV panels or shadow modeling, thus generally overestimating the PV generation potential. However, even when these aspects are taken into account, existing literature shows that the inclusion of PV panels from different oriented roofs and facades can be beneficial for matching electrical demand profiles. [13], based on the case study of two building blocks in Portugal, showed the economic feasibility of facades and demonstrated that including facades has a minimizing effect on the required storage size.

To expand the scope from single buildings to whole districts, 3D simulation software using ray tracing technique like LiDAR in combination with geographic information systems (GIS) tools was developed [14, 15, 16] and commonly used to access solar potential on all surfaces in a district [17, 18, 19]. The use of these tools also allowed for the inclusion of surrounding buildings in the model, a necessary condition include the effect of shading on the potential for PV generation from facades. In addition, *Sky view factor* is a commonly used indicator for determining the amount of diffuse irradiation on the surface [20, 21], whose use becomes even more relevant in the case of PV systems on facades.

The solar potential on facades is in general lower than on roofs [22]. However, previous research also suggested some potential advantages. [14] showed that the combined PV potential on roofs and facades exceeds the non-baseload demand for a district located in Portugal and could furthermore contribute up to 75% of the total electrical demand. Also [23] suggested to take PV installation on facades into account, especially for high rise buildings. Also [24] and [25] conclude that facade installation can be competitive with roof installation whereas [14] suggest to first exploit roofs before starting installing PV panels on facades.

The potential for facades also strongly depends on the location: [26], based on the results of a case-study application in Germany, suggested that the solar potential on facades can exceed that on roofs during the winter months, as a result of the sun being low in the sky. Consistently, rooftop solar is economically superior to facades, as in the latter case the payback increased from 10 to 20 year. Clearly, the orientation of the surface also has a role in the performance of the system. As a relevant example, [27] determine a 12 year carbon - and a 10 year payback time of PV panels mounted on South oriented facades in Serbia.

# 5. Materials and methods

To be able to take both, the optimal integration at building level and the behaviour of the whole district into account, a mixed-integer linear programming (MILP) framework is formulated, where unit sizes and installation decisions in each building as main optimization variables. The approach is based on the general formulation of the BES, which can be then applied to different building types in a district. The model derives from the BES framework described by [28], to which the reader is referred for further details. In this paper, a special attention is dedicated to the further development of the oriented irradiation modelling proposed in earlier work from the authors [8], which is modified so to include the modelling of shading effects between different buildings in the districts.

To clearly differentiate decision variables from input parameters, bold typeset is used to represent all decision variables. Additional parameter values can be found in the Supplementary Material. The main sets that are used to define the problem are the set of of buildings **B** and their allocated Facades **F**, possible conversion and storage units **U**,different discrete temperature levels**K**, different days of the year represented by periods in the set **P**, to which hourly timesteps are allocated and contained in set **T**.

The BES modeling framework includes multiple unit technologies that can contribute to satisfy the different energy demands (Figure 1). Both the space heating space heating (SH) and domestic hot water (DHW) demands can be fulfilled by a gas boiler, converting natural gas into thermal energy, or by heat pumps and electrical heaters, both converting electricity to thermal energy. PV panels are also considered as energy conversion units, converting incoming solar irradiation to electricity. The system also includes storage technologies. Two different tanks are considered, one for SH and one for DHW, as thermal energy storage systems. Electric energy storage is also considered in the form of lithium ion batteries.

In the proposed models, buildings are differentiated not only based on their constructive characteristics (surface, volume, roof type, etc) but also by their usage, such as residential or industrial, which mostly influences the energy demand profiles, by and their renovation state.

## 5.1. Problem objectives

The MILP problem is defined with the minimization of the BES costs as the main problem objective. This involves the combination of two separate contributions: operating and capital expenses. As these two objectives are generally competing (solutions with high capital expenses (CAPEX) have low operational expenses (OPEX), and vice versa), the problem must be approached using a multi-objective optimization (MOO) approach. The MOO problem is implemented using the $\epsilon$-constraint method, thus considering the OPEX as the main problem objective and solving different optimization problems where the CAPEX is constrained at incrementally increasing values. The same principle is then repeated after inverting the roles of the two objectives.

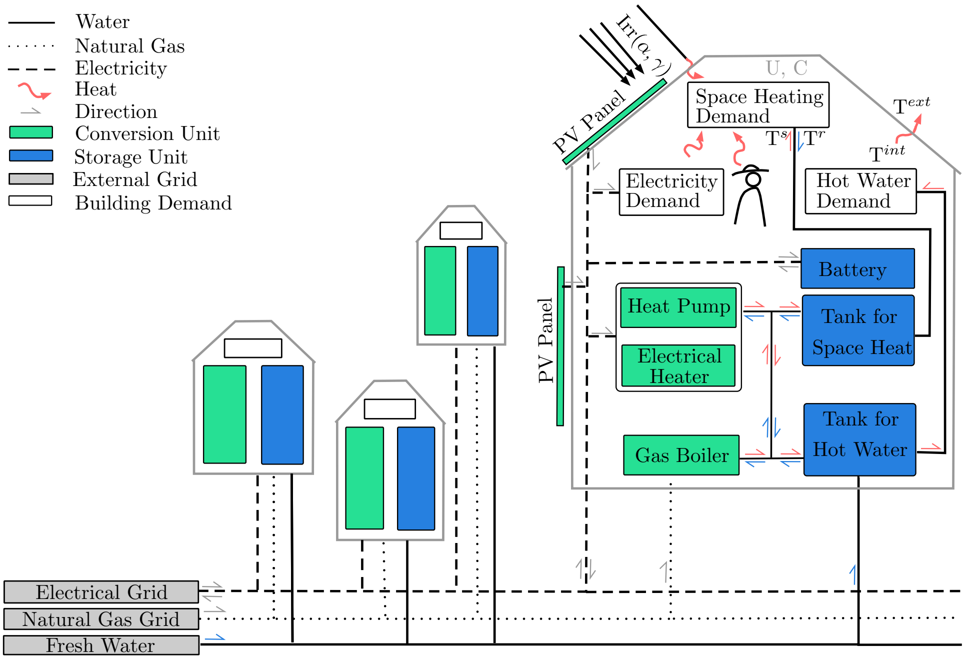


*Figure 1: Overview of District Energy System. $U, C$ Building heat transfer and capacity factor, $Irr$ irradiation, $T$ Temperatures.*

The annual OPEX consist of the expenses and gains related to the interaction with the national electric and natural gas grids, as shown in Equation 1. $c^{el,+}$, $c^{el,-}$ and $c^{ng,+}$ represent the electricity purchase and selling price, and the natural gas purchase price; $\dot{H}^{gr,+}_{b,p,t}$ represents the energy flow of natural gas purchased from the grid for building $b$ at time step $t$ and typical day $p$; similarly,$\dot{\boldsymbol{E}}^{\boldsymbol{gr,+}}_{\boldsymbol{b,p,t}}$ and $\dot{\boldsymbol{E}}^{\boldsymbol{gr,-}}_{\boldsymbol{b,p,t}}$ represent the electric energy flows from and to the grid. Annual values are integrated over each typical period $p$ and accounted with their frequency $d$.

$$\boldsymbol{C}^{op}_b = \sum_{p \in \mathbf{P}} \sum_{t \in \mathbf{T}} \left( c^{el,+} \cdot \dot{\boldsymbol{E}}^{\boldsymbol{gr,+}}_{\boldsymbol{b,p,t}} - c^{el,-} \cdot \dot{\boldsymbol{E}}^{\boldsymbol{gr,-}}_{\boldsymbol{b,p,t}} + c^{ng,+} \cdot \dot{\boldsymbol{H}}^{\boldsymbol{gr,+}}_{\boldsymbol{b,p,t}} \right) \cdot d_t \cdot d_p \quad \forall b \in \mathbf{B} \tag{1}$$

The annual CAPEX include the investment and replacement costs of the unit technologies with different expected lifetimes. The costs are annualized over the project time horizon $n$ using the project interest rate $i$ [29, Ch. 10 ]. The parameters $i^{c1}$ and $i^{c2}$ represent the linear version of the unit cost function with bare module $b^u$ [28]. If the project horizon exceeds the lifetime of a unit ($l^u$), the unit must be replaced and purchased again (Equation 2c). For units with a lifetime greater than or equal to the project time horizon, the total number of replacements ($R$) is zero. [28]

$$\boldsymbol{C}^{cap}_b = \frac{i(1+i)}{(1+i)^n - 1} \left( \boldsymbol{C}^{inv}_b + \boldsymbol{C}^{rep}_b \right) \tag{2a}$$

$$\boldsymbol{C}^{inv}_b = \sum_{u \in \boldsymbol{U}} b_{b,u} \cdot \left( i^{c1}_{b,u} \cdot \boldsymbol{y_{b,u}} + i^{c2}_{b,u} \cdot \boldsymbol{f_{b,u}} \right) \tag{2b}$$

$$\boldsymbol{C}^{rep}_b = \sum_{u \in \boldsymbol{U}} \sum_{r \in \boldsymbol{R}} \frac{1}{(1+i)^{r \cdot l_u}} \cdot \left( i^{c1}_{b,u} \cdot \boldsymbol{y_{b,u}} + i^{c2}_{b,u} \cdot \boldsymbol{f_{b,u}} \right) \quad \forall b \in \mathbf{B} \tag{2c}$$

## 5.2. Key performance indicators

In addition to the problem objectives, key performance indicator (KPI)s are defined to provide additional information regarding the performance of the system. For readability, the following equations are expressed with annual values.

The self-consumption (SC), the self-sufficiency (SS) and the photovoltaic penetration (PVP) are KPIs used to evaluate the performance of the system in terms of its interaction with the grid. The SC represents the share of the generated electricity from all PV panels $\boldsymbol{E^{pv,+}}$ consumed within the district (Equation 3a) [30]; the SS represents the ratio of the onsite generated electricity consumption to the total electricity demand (Equation 3b) [30]; finally. the PVP measures how much of the total electricity demand could be covered by generated electricity from photovoltaic panels (Equation 3c). Unlike the SS and SC, PVP does not evaluate the share of generated electricity consumed on site.

$$SC = \frac{(\sum_{b \in \mathbf{B}} \boldsymbol{E_b^{pv,+}}) - \boldsymbol{E^{TR,-}}}{(\sum_{b \in \mathbf{B}} \boldsymbol{E_b^{pv,+}})} \tag{3a}$$

$$SS = \frac{(\sum_{b \in \mathbf{B}} \boldsymbol{E_b^{pv,+}}) - \boldsymbol{E^{TR,-}}}{(\sum_{b \in \mathbf{B}} \boldsymbol{E_b^{pv,+}}) - \boldsymbol{E^{TR,-}} + \boldsymbol{E^{TR,+}}} \tag{3b}$$

$$PVP = \frac{(\sum_{b \in \mathbf{B}} \boldsymbol{E_b^{pv,+}})}{(\sum_{b \in \mathbf{B}} \boldsymbol{E_b^{pv,+}}) - \boldsymbol{E^{TR,-}} + \boldsymbol{E^{TR,+}}} \tag{3c}$$

Additional KPIs are used to evaluate how the system performs in terms of Greenhouse gas (GHG) emissions, here included based on their $CO_2$ equivalence [10]. In latter approach, the footprint of batteries and thermal storage cannot be considered. In this study, the total global warming potential (GWP) is divided into the share coming from the operation $G^{op}$ and the construction of the BES $G^{bes}$ to derive the annual global warming potential $G^{lca}$, as shown in Equation 4.

$$\boldsymbol{G}^{lca} = \boldsymbol{G}^{bes} + \boldsymbol{G}^{op} \tag{4}$$

Equation 5 shows how the GWP from the system's operations is calculated, where the period and time-dependent emission parameters $g_{p,t}$ are accounted for the GWP per kWh consumed electricity $E$ [31] or natural gas $H$. The parameter $d_t$ accounts for the duration of each timestep within a period and $d_p$ for the duration or frequency of each period within one year.

$$\boldsymbol{G}^{op} = \sum_{p \in \boldsymbol{P}} \sum_{t \in \boldsymbol{T}} \left( g_{p,t}^{el} \cdot \boldsymbol{E}_{p,t}^{TR,+} - g_{p,t}^{el} \cdot \boldsymbol{E}_{p,t}^{TR,-} + g^{ng} \cdot \sum_{b \in \boldsymbol{B}} \dot{\boldsymbol{H}}_{b,p,t}^{gr,+} \right) \cdot d_p \cdot d_t \tag{5}$$

The database Ecoinvent [32] documents the environmental impact of energy processes and materials and provides life cycle assessments of the different technologies. To assess the GWP of different unit technologies, the indicator "GWP 100a" of the method "IPCC 2013" documented in the online version 3.6 of ecoinvent is adopted. This indicator considers GHG emissions based on the GWP published by the

Intergovernmental Panel on Climate Change (IPCC) for a time horizon of 100 years. The GWP of different unit technologies $\boldsymbol{G}^{bes}$ is expressed in Equation 6.

$$\boldsymbol{G}^{bes} = \sum_{b \in \boldsymbol{B}} \sum_{u \in \boldsymbol{U}} \frac{1}{l_u} \cdot \left( i_u^{g1} \cdot \boldsymbol{y_{b,u}} + i_u^{g2} \cdot \boldsymbol{f_{b,u}} \right) \tag{6}$$

In addition to the total GWP of the system, the carbon payback time Carbon Payback Time (CPT) is used as an additional KPI of the system. calculated based on the indirect emissions of all PV panels, which are installed in the district $G^{bes,pv}$, and the avoided emission while operating them (Equation 7) [33].

$$\boldsymbol{G}^{pbt} = \frac{\boldsymbol{G^{bes,pv}}}{\sum_{b \in \boldsymbol{B}} \sum_{p \in \boldsymbol{P}} \sum_{t \in \boldsymbol{T}} (g_{p,t}^{el} \cdot \boldsymbol{E_{b,p,t}^{pv,+}}) \cdot d_t \cdot d_p} \tag{7}$$

## 5.3. Energy demand

As this study aims at estimating the extent to which decentralized renewable energy generation can be integrated in the building stock, all types of energy demand related to building energy systems are considered. As illustrated in Figure 1, three types of energy demands are considered in the model: space heatingSH, domestic hot water DHW, and electricity. The electricity and especially the space heating demand are influenced by the renovation state of the building, while the demand of DHW is fixed.

### Space Heating demand

The general form of the space heating demand can be expressed by the thermal balance Equation 8, where the three terms of the addition represent the internal heat gains from appliances, people and solar irradiation ($Q^{gain}$), the heat transfer by conduction and air renewal ($\boldsymbol{\dot{Q}_{b,p,t}^{CAR}}$) and the heat stored in the thermal inertia of the building ($\boldsymbol{\dot{Q}_{b,p,t}^{BTI}}$) [28].

In this study, the internal building temperature $\boldsymbol{T^{int}}$ is considered as a variable to be optimized. This allows the building heat capacity to work as an additional, free thermal storage for the building energy system, thus making it possible to use available surplus electricity from PV modules. Clearly, comfort should also be taken into account: this is done through the introduction of a penalty cost in the optimization problem objective of 5 CHF/K per hour when the indoor temperature exceeds pre-defined bounds.

$$\boldsymbol{\dot{Q}_{b,p,t}^{SH}} = \dot{Q}_{b,p,t}^{gain} - \boldsymbol{\dot{Q}_{b,p,t}^{CAR}} - \boldsymbol{\dot{Q}_{b,p,t}^{BTI}} \quad \forall b \in \mathbf{B} \quad \forall p \in \mathbf{P} \quad \forall t \in \mathbf{T} \tag{8}$$

$$\boldsymbol{\dot{Q}_{b,p,t}^{CAR}} = U_b \cdot A_b^{th} \cdot (\boldsymbol{T_{b,p,t}^{int}} - T_{p,t}^{ext}) \quad \forall b \in \mathbf{B} \quad \forall p \in \mathbf{P} \quad \forall t \in \mathbf{T} \tag{9}$$

$$\boldsymbol{\dot{Q}_{b,p,t}^{BTI}} = C_b \cdot A_b^{th} \cdot (\boldsymbol{T_{b,p,t+1}^{int}} - \boldsymbol{T_{b,p,t}^{int}}) \quad \forall b \in \mathbf{B} \quad \forall p \in \mathbf{P} \quad \forall t \in \mathbf{T} \tag{10}$$

$$\dot{Q}_{b,p,t}^{gain} = \dot{Q}_{b,p,t}^{int} + \dot{Q}_{b,p,t}^{irr} \quad \forall b \in \mathbf{B} \quad \forall p \in \mathbf{P} \quad \forall t \in \mathbf{T} \tag{11}$$

In this study, the SH thermal load $\boldsymbol{\dot{Q}^{SH}}$ is considered as a variable, as it depends on the indoor temperature (see Equations 9 and 10) .

The $\dot{\boldsymbol{Q}}^{\boldsymbol{CAR}}_{\boldsymbol{b,p,t}}$ term in equation 8 represents the heat transfer by conduction and air renewal. The heat transfer coefficient $U$ is different for each building, and represents a combination of heat losses through the building envelope (walls, windows, roofs) and of ventilation losses.

The $\dot{\boldsymbol{Q}}^{\boldsymbol{BTI}}_{\boldsymbol{b,p,t}}$ term in equation 8 represents the contribution to the heat balance connected to the charge/discharge of the heat stored as thermal energy in the building walls. The thermal heat capacity $C$ describes the thermal inertia of the building. $A^{th}$ is the thermal surface, also known as energetic reference area, which has to be heated.

The heat gain term is composed of two contributions: internal gains resulting from the usage of the building ( $\dot{Q}^{int}$), and solar irradiation ($\dot{Q}^{irr}_{b,p,t}$).

$$\dot{Q}^{int}_{b,p,t} = A^{net}_b \cdot \sum_{r \in Rooms} f_{b,r} \cdot f^u_{r,p} \cdot (\Phi^P_{r,p,t} + \Phi^{A+L}_{r,p,t}) \quad \forall b \in \textbf{B} \quad \forall p \in \textbf{P} \quad \forall t \in \textbf{T} \tag{12}$$

The internal gains are mainly the immediate consequence of the occupancy of the people (superscript $P$) and the usage of electric appliances and lights (superscript $A+L$). Demand profiles for the different building and room usages are taken from the Swiss standard norm [34]. The total gains for each building result from the sum of the gains of each room of the building (Equation 12). A usage factor $f^u$ is used to account for monthly/weekly variations related to the specific usage of each building and room type [34].. The internal gains, are normalized to the internal net surface of the building $A^{net}$, calculated as the heated surface without the base surface of inner and outer walls.

The heat gain from solar irradiation (see Equation 13) is calculated based on the Swiss technical norm [34], where the solar gain factor $\psi$ is calculated in a preprocessing step. The global irradiation $irr$ is calculated as a function of time as described in 5.5, while the the total heated surface $A^{th}$ of the building is calculated based on the knowledge of the building's geometry.

$$\dot{Q}^{irr}_{b,p,t} = \psi_b \cdot A^{th}_b \cdot irr_{p,t} \quad \forall b \in \textbf{B} \quad \forall p \in \textbf{P} \quad \forall t \in \textbf{T} \tag{13}$$

### Domestic hot water demand

Typical DHW demand is stated in standardized national norms [34, 35]. Similar to the internal heat gains, the DHW profile is specific to each room type and usage. The factor $n_p/A^{net}_r$ expresses the number of reference units per net surface of the specific room (Equation 14).

$$Q^{dhw}_b = A^{net}_b \cdot \sum_{r \in Rooms} f_{b,r} \cdot f^u_{r,p} \cdot V^{dhw,P}_r \cdot \frac{n_P}{A^{net}_r} \cdot c^{dhw}_p \cdot \rho^{dhw}(T^{dhw} - T^{cw}) \quad \forall b \in \textbf{B} \tag{14}$$

The cold water temperature is assumed to be constant at $T^{cw} = 10$°C, whereas the hot water temperature has to be delivered at $T^{dhw} = 60$°C to meet sanitary standards. The thermodynamic properties

$(\rho \cdot c_p)^{dhw}$ are the density and the specific heat capacity of water. The daily profiles are derived from the occupancy profiles in combination with the activity profiles of the rooms.

### Electricity Demand

Two different methods are used to estimate the electricity demand, based on the availability of measurements from the existing buildings.

When measurements are available, the electricity demand is calculated as the difference between the measured electricity demand and the calculated heating demand [36]. When measured data is not available, the electricity demand is calculated based on the profiles provided by the Swiss standard norm [34]. The electricity demand of the appliances and light of the different rooms are combined in the $E^{A+L}$ term (Equation 15). The $A_b^{net}$, $f_{b,r}$ and $f_{r,p}^u$ factors are the same used to calculate the domestic hot water demand.

$$\dot{E}^B_{b,p,t} = A_b^{net} \cdot \sum_{r \in Rooms} f_{b,r} \cdot f^u_{r,p} \cdot \dot{E}^{A+L}_{r,p,t} \quad \forall b \in \mathbf{B} \quad \forall p \in \mathbf{P} \quad \forall t \in \mathbf{T} \tag{15}$$

## 5.4. Energy system

The energy system of the building includes all the different unit technologies that are used to fulfil the building's energy demand (see Equation 16). The superscript $+$ indicates outgoing flows like the supply of each grid or unit, whereas $-$ marks an incoming flow, also often refereed to as demand unit or feed–in to the grids. The heat cascade ensures that heat requirements are supplied, while the second law of thermodynamic is satisfied (Equation 16c and 16d). In Equation 16c the residual heat $R_k$ is cascaded to the next interval ($k+1$). Equation 16d closes the thermal balance by ensuring that no heat cascaded to the highest or lowest interval [28].

$$\dot{\boldsymbol{E}}^{\boldsymbol{gr,+}}_{\boldsymbol{b,p,t}} + \sum_{u \in \mathbf{U}} \dot{\boldsymbol{E}}^{+}_{\boldsymbol{b,u,p,t}} = \dot{\boldsymbol{E}}^{\boldsymbol{gr,-}}_{\boldsymbol{b,p,t}} + \sum_{u \in \mathbf{U}} \dot{\boldsymbol{E}}^{-}_{\boldsymbol{b,u,p,t}} + \dot{E}^B_{b,p,t} \tag{16a}$$

$$\dot{\boldsymbol{H}}^{\boldsymbol{gr,+}}_{\boldsymbol{b,p,t}} = \sum_{u \in \mathbf{U}} \dot{\boldsymbol{H}}^{-}_{\boldsymbol{b,u,p,t}} \tag{16b}$$

$$\dot{\boldsymbol{R}}_{\boldsymbol{k,b,p,t}} - \dot{\boldsymbol{R}}_{\boldsymbol{k+1,b,p,t}} = \sum_{u_h \in \boldsymbol{U}} \dot{\boldsymbol{Q}}^{-}_{\boldsymbol{u_h,k,b,p,t}} - \sum_{u_c \in \boldsymbol{U}} \dot{\boldsymbol{Q}}^{+}_{\boldsymbol{u_c,k,b,p,t}} \tag{16c}$$

$$\dot{\boldsymbol{R}}_{\boldsymbol{1,b,p,t}} = \dot{\boldsymbol{R}}_{\boldsymbol{n_k+1,b,p,t}} = 0 \tag{16d}$$

$$\forall k \in \mathbf{K} \quad \forall b \in \mathbf{B} \quad \forall p \in \mathbf{P} \quad \forall t \in \mathbf{T}$$

Energy can be exchanged with the electricity grid $E^{gr}$ in both ways (Equation 16a), whereas water and gas grids $H$ can only supply (Equation 16b). To account for the possibility that electricity can generated and consumed in the district itself, Equation 17 balances loads at transformer level (superscript $TR$ )of the district.

$$\dot{\boldsymbol{E}}_{\boldsymbol{p,t}}^{\boldsymbol{TR,+}} - \dot{\boldsymbol{E}}_{\boldsymbol{p,t}}^{\boldsymbol{TR,-}} = \sum_{b \in \mathbf{B}} \dot{\boldsymbol{E}}_{\boldsymbol{b,p,t}}^{\boldsymbol{gr,+}} - \sum_{b \in \mathbf{B}} \dot{\boldsymbol{E}}_{\boldsymbol{b,p,t}}^{\boldsymbol{gr,-}} \quad \forall p \in \mathbf{P} \quad \forall t \in \mathbf{T} \tag{17}$$

To ensure that no energy is accumulated between different periods, cyclic constraints are imposed both on the indoor temperature and on thermal and electrical energy storage systems. Cyclic constraints ensure that the state is reset to its initial status at the end of each period.

The main equation for sizing and scheduling problem units are described by Equations 18. The decision to purchase a unit is represented by the binary variable $\boldsymbol{y_u}$, whereas the continuous variable $\boldsymbol{f_u}$ represents the unit size. The reader should refer to [28] for the full description of the energy systems modeled in this study.

$$\boldsymbol{y_{b,u}} \cdot F_u^{min} \leq \boldsymbol{f_{b,u}} \leq \boldsymbol{y_{b,u}} \cdot F_u^{max} \tag{18a}$$

$$\boldsymbol{f_{b,u,p,t}} \leq \boldsymbol{f_{b,u}} \tag{18b}$$

$$\boldsymbol{y_{b,u,p,t}} \leq \boldsymbol{y_{b,u}} \tag{18c}$$

$$\forall b \in \mathbf{B} \quad \forall u \in \mathbf{U} \quad \forall p \in \mathbf{P} \quad \forall t \in \mathbf{T}$$

For facades Fmax is not big enough for PV. Since smal PV installation on roof should also be possible we need piecewise lineraization

$$\boldsymbol{C_b^{inv,pv}} = \sum_{i \in \boldsymbol{I}} b_{b,u,i} \cdot \left( i_{b,u,i}^{c1} \cdot \boldsymbol{y_{b,u,i}} + i_{b,u,i}^{c2} \cdot \boldsymbol{f_{b,u,i}} \right) \tag{19a}$$

$$\boldsymbol{y_{b,u}} = \sum_{i \in \mathbf{I}} \boldsymbol{y_{b,u,i}} \tag{19b}$$

$$\boldsymbol{f_{b,u}} = \sum_{i \in \mathbf{I}} \boldsymbol{f_{b,u,i}} \tag{19c}$$

$$\boldsymbol{y_{b,u,i}} \cdot F_{u,i}^{min} \leq \boldsymbol{f_{b,u,i}} \leq \boldsymbol{y_{b,u,i}} \cdot F_{u,i}^{max} \tag{19d}$$

$$F_{u,i=0}^{min} = F_u^{min} \tag{19e}$$

$$F_{u,i=n}^{min} = F_u^{max} \tag{19f}$$

$$\forall i \in \mathbf{I} \quad \forall b \in \mathbf{B} \quad \forall u = pv$$

## 5.5. Solar irradiation

The hourly irradiation is modeled using the anisotrop irradiation model which is first stated by [37] and further improved for all sky conditions [38]. The skydome descritization [39] is applied using the Ladybug plug-in of the Grasshopper suite [40] to include the oriented irradiation into a MILP formulation. For more information about modeling oriented irradiation in MILP problems, the reader should refer to [8], while in the remaining part of this section the focus will shift to facades, the main element of novelty in this work.

Compared to roofs, the direct solar irradiation on facades highly depends on shading from neighbouring buildings, making it necessary to include a detailed shadow modelling.

The shadow modelling employed in this study only includes the shadow from surrounding buildings, not from other obstacles (such as trees). Figure 2 visualizes an exemplary geometric relation between two Buildings. The positions of buildings and facades are given in x,y z coordinates where y points North, x

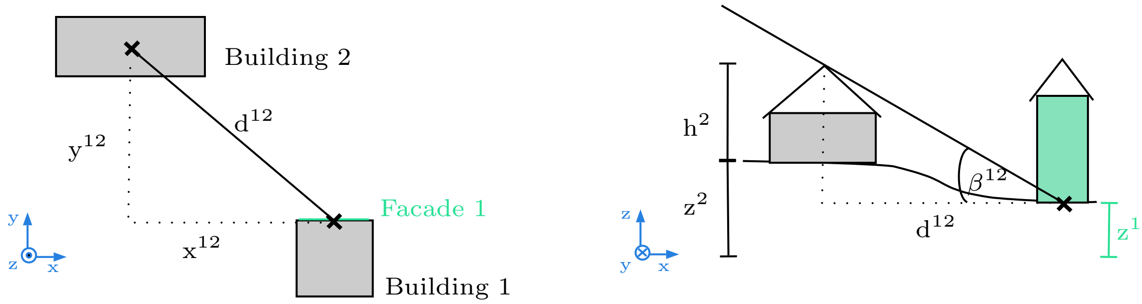


*Figure 2: Exemplary visualization of the geometry for Facade 1, with distance $d^{12}$ to Building 2 and the sky limiting angle $\beta$.*

East and z the elevation. The assumption is that the shortest distance is between the center point of the facades and the center point of the building (Figure 2). Equations 20 show how the distance between buildings $b$ and facades $f$ in x and y coordinates is calculated.

$$x^{f,b} = |x^b - x^f| \tag{20a}$$

$$y^{f,b} = |y^b - y^f| \qquad \forall f \in \mathbf{F}, b \in \mathbf{B} \tag{20b}$$

$$d^{f,b} = \sqrt{(y^{f,b})^2 + (x^{f,b})^2} \qquad \forall f \in \mathbf{F}, b \in \mathbf{B} \tag{20c}$$

The sky limiting angle $\beta$ represents the lowest elevation angle from which irradiation reaches the facades (Figure 2). The reference point for the sky limiting angle is the bottom of each facade. This is considered a conservative assumption in order not to overestimate the energy generated by PV panels installed on facades.

$$\tan(\beta^{f,b}) = \frac{h^b + z^b - z^f}{d^{f,b}} \qquad \forall f \in \mathbf{F}, b \in \mathbf{B} \tag{21}$$

The sky direction is expressed by the azimuth angle $\alpha$, which is 0°for North direction and 180°for South orientation. Figure 3 shows the different azimuth angles of the facades, surrounded buildings and sky-dome patches.

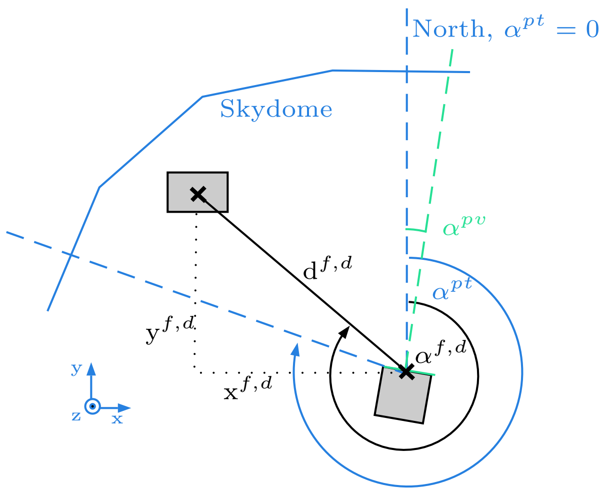


*Figure 3: Outline sketch of different azimuth angles. The azimuth orientation of the facades are identical to possible PV modules $\alpha^{PV}$. $\alpha^{f,b}$: azimuth direction of surrounding buildings, $\alpha^{pt}$: azimuth direction of each patch of the skydome .*

Equation 22 shows how the azimuth position of building $b$ is calculated. Knowing the signs of both catheti makes it possible to assess the correct quadrant for azimuth angle $\alpha^{f,b} \in [0°, 360°]$.

$$\alpha^{f,b} = \arctan\left(\frac{x^b - x^f}{y^b - y^f}\right) \qquad \forall f \in \mathbf{F}, b \in \mathbf{B} \tag{22}$$

The sky limiting angle $\beta$ is greatest in the azimuth direction $\alpha^{f,b}$ of the building causing the shadow. As a building is affected by a range of azimuth angles the sky limiting angle is calculated for all azimuth angles $\alpha^{pt}$ of the sky dome patches $pt$ (see Equation 23).

$$\tan(\beta^{f,b,\alpha}) = \frac{h^b + z^b - z^f}{d^{f,b}} \cdot \cos(\Delta\alpha) = \tan(\beta^{f,b}) \cdot \cos(\alpha^{f,b} - \alpha^{pt}) \qquad \forall f \in \mathbf{F}, b \in \mathbf{B}, \forall pt \in \mathbf{P} \tag{23}$$

Finally, the highest sky limiting angle $\beta^{f,\alpha}$ in each azimuth direction $\alpha^{pt}$ of the skydome is selected among all surrounding buildings for each facade $f$ (Equation 24).

$$\beta^{f,\alpha} = \max\{\beta^{f,b,\alpha} : b \in \mathbf{B}\} \quad \forall f \in \mathbf{F}, \alpha^{pt} | pt \in \mathbf{P} \tag{24}$$

The sky limiting angle in each azimuth direction is then used to determine the shaded irradiation. Thereby the method is similar to the calculation of inter-modular shading of PV modules on flat roofs [8]. The skydome is piecewise linerized over the evaluation angle of one patch, which varies 12°, with $\epsilon^{pt}$ marking the central point (Equation 25) of each patch. The resulting shading factor of of one patch $s^{pt} \in [0; 1]$ is equal to zero for completely shaded patches, 1 for completely unshaded patches.

$$s^{f,pt} = \begin{cases} 0 & \epsilon^{pt} \leq \beta^{f,\alpha} \\ \frac{\epsilon^{pt}+6-\beta^{f,\alpha}}{12} & \beta^{f,\alpha} - 6 < \epsilon^{pt} < \beta^{f,\alpha} + 6 \\ 1 & \epsilon^{pt} \geq \beta^{f,\alpha} + 6 \end{cases} \quad \forall f \in \mathbf{F}, (\alpha^{pt}, \epsilon^{pt}) | pt \in \mathbf{P} \tag{25}$$

Equation 26 finally shows how the irradiation on facades is calculated when taking into account shading from neighbouring buildings. As possible panels can only take the orientation of the facades, the azimuth and tilt orientation of the facades are equivalent to the orientation of the PV panel. In contrast to the azimuth angle, tilt angle of the facades is always the same $\gamma^{pv} = 90°$. The oriented irradiation $irr(\alpha, \gamma)$ of each patch $pt$ of the skydome on the PV panel is calculated using the principle of a two stage rotation in a three dimensional space, which is treated in detail in [8].

$$\begin{aligned} irr^{f,pv}(\alpha^{pv}, \gamma^{pv}) =& (-1) \cdot \sum_{pt \in \boldsymbol{P}} s^{f,pt} \cdot irr^{pt}(\alpha^{pv}, \gamma^{pv}) \\ & \forall \alpha^{pv} \in \mathbf{A}, \forall \gamma^{pv} \in \mathbf{T} \end{aligned} \tag{26}$$

## 5.6. Generation and Aggregation of Input data

Azimuth angles in Swissbuilding3D and Sonnendach: north -180, east -90, south 0, west 90. This study uses: north 0, east 90, south 180, west 270.
Unison decision for tilt angle = 0 is horizontal, 90 vertical. $x^{sd}$ points to the east , $y^{sd}$ to the north and $z^{sd}$ to the zenith, and the azimuth angle increases clockwise starting from the north, where $\alpha = 0$. The elevation angle and tilt angle increases counterclockwise from $\epsilon = 0, \gamma = 0$ for patches with no elevation in the sky.

# 6. Case study

## 6.1. Data driven approach

The data layers of Table 1 are used to represent the multiple configurations of decentralised energy demand and generation. Except for the grid topology and measurement [36], the approach uses Open Government Data (OGD) including the climatic conditions, building database[41] with roof and facade geometries [42, 43], energy demand standards [44, 34] and statistical values [45].

*Table 1: List of the necessary data layers*

| Type | Data | Description |
|---|---|---|
| Environment | Weather data | Temperature and solar irradiation [46, 47] |
| Land registery | Cadastre | Footprint area [48, 49] |
| Buildings | Official Buildings Registry | Usage, construction/renovation date, heating system, height, number of floor, reference energy area [50, 41] |
| | 3D model | 3D surfaces[42] |
| | Solar roof and facade | 2D surfaces area and orientation [43, 51] |
| | Energy statistics and standards | Overall heat transfert coefficient, heat capacity, people presence, electrical loads, internal and external gain [44, 34] |
| Grid | Grid topology | Transformers, lines & injection points [52] |
| | Load measurements | Hourly load at the transformer [52, 36] |

The optimisation is performed using a selection of 10 typical days of 24 hours presented in Table 2.

*Table 2: Typical days used for the g*

| # | Date | Day | Frequency |
|---|---|---|---|
| 1 | 02/22 | 53 | 59 |
| 2 | 02/14 | 45 | 46 |
| 3 | 02/09 | 40 | 23 |
| 4 | 05/01 | 121 | 35 |
| 5 | 10/05 | 278 | 40 |
| 6 | 04/06 | 96 | 37 |
| 7 | 05/14 | 134 | 16 |
| 8 | 08/26 | 238 | 42 |
| 9 | 09/18 | 261 | 24 |
| 10 | 08/17 | 229 | 43 |

## 6.2. Description

The method is demonstrated on the RE demo peri-urban residential areas comprising 31 buildings, mostly single and multi-family houses, connected to the same measured transformers (Figure 4a). The buildings considered are all connected to the same measured transformer (TR3716), the other buildings of the district being solely used for their shadowing effect.

Figure 4b shows that, with the building roofs hosting 30% of the available PV area and 48% of the generation potential, facades represent a significant generation potential. As expected, South-oriented facades have the largest potential, followed by East- and West-oriented facades. It is interesting to notice that the specific solar potential of the most promising South-oriented facades is higher than that of the least promising roofs.

The main characteristics of the building stock of the district, including typology, form, annual energy demand and physical parameters are summarized in Table 3.

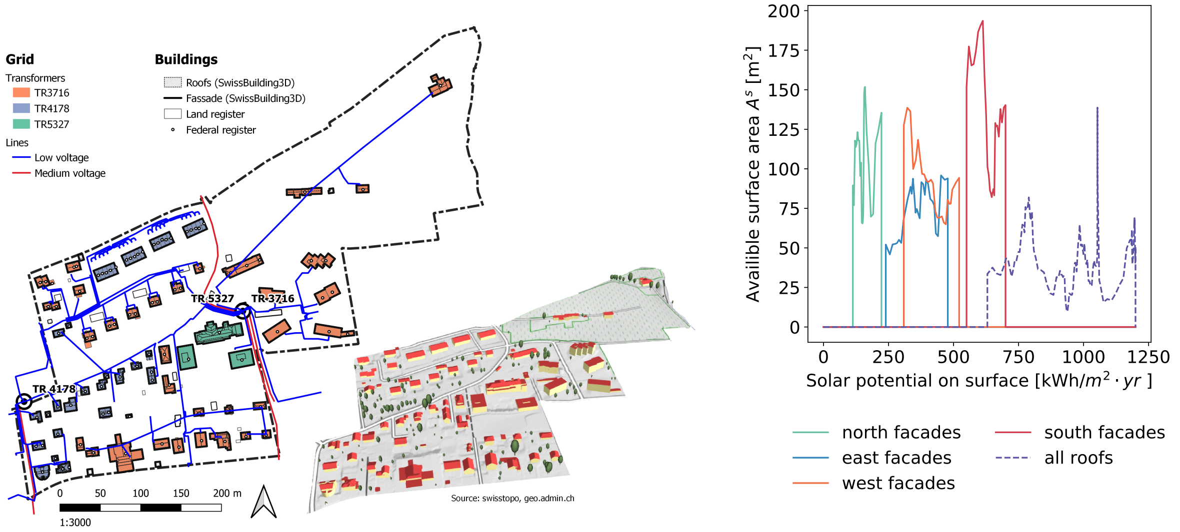


*(a) Peri-urban residential areas*

*(b) PV potential on roof and facade*

*Figure 4: Map of the case study area (a) with the PV potential on roof and different orientation of facades (b)*

*Table 3: Characteristics of the building stock. All buildings are connected to the same low voltage grid.*

| | | Multi family house | Multi family house | Single family house | |
|---|---|---|---|---|---|
| Building type $^+$ | | I | I | II | |
| Building category$^+$ | | existing | standard | existing | |
| Number of buildings | | 11 | 2 | 18 | |
| Total net surface | $A^{net}$ | 9200 | 1100 | 5600 | m$^2$ |
| Total energy ref. area | $A^{th}$ | 11500 | 1400 | 7000 | m$^2$ |
| Total roof area$^\star$ | $A^s$ | 4200 | 560 | 4400 | m$^2$ |
| Total facades area$^\star$ | $A^s$ | 7700 | 870 | 5900 | m$^2$ |
| Annual electricity demand$^\dagger$ | $E^B$ | 37 $\pm$ 17 | 50 $\pm$ 21 | 60 $\pm$ 60 | kWh/m$^2_{net}$ |
| Annual hot water demand$^\dagger$ | $Q^{dhw}$ | 25$\pm 0$ | 25$\pm 0$ | 19$\pm 0$ | kWh/m$^2_{net}$ |
| Annual internal heat gain$^\dagger$ | $Q^{int}$ | 30 $\pm 2$ | 32 $\pm 0$ | 29 $\pm 2$ | kWh/m$^2_{net}$ |
| Solar heat gain$^\dagger$ | $Q^{irr}$ | 22 $\pm 6$ | 20 $\pm 3$ | 31 $\pm 10$ | kWh/m$^2_{th}$ |
| Design Supply Temperature | $T_0^s$ | 65 | 41.5 | 65 | °C |
| Design Return Temperature | $T_0^r$ | 50 | 33.9 | 50 | °C |
| Heat transfer factor$^\dagger$ | $U$ | 1.74 $\pm 0.24$ | 0.83 $\pm 0$ | 1.84 $\pm 0.21$ | W/(m$^2_{th}$ K) |
| Heat capacity factor$^\dagger$ | $C$ | 118 $\pm 5$ | 120 $\pm 0$ | 120$\pm 0$ | Wh/(m$^2_{th}$ K) |

$^+$ according Swiss standard norm [34]

$^\star$ Area available for PV installation. Details available in [53].

$^\dagger$ Average values $\pm$ standard deviation.

# 7. Results

The optimal solutions shown in Figure 5 results from the parametric multi-objective optimisation of the model with the actual feed-in cost of 8 cts/kWh and purchase electricity tariff of 20 cts/kWh. Low investment (CAPEX) and high operating (OPEX) cost solutions are located on the left side of the x-axis, while increasingly self-sufficient decentralised solutions, with higher investment and lower operating cost, are located on the left.

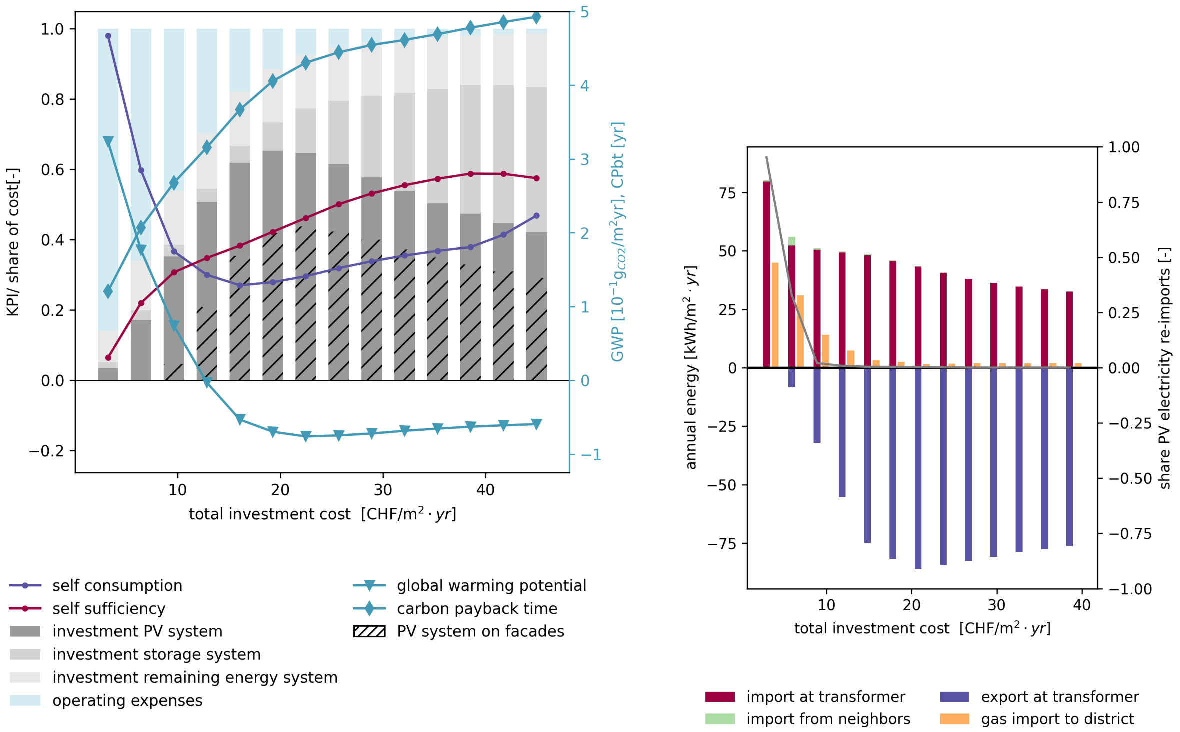


*(a)* *(b)*

*Figure 5: Results of the MOO of 31 buildings in one low voltage grid. a) performance indicators and cost distribution of identified energy systems b) electricity exchange and gas imports for the district.*

## 7.1. Self-sufficiency and carbon-neutrality

The results of the optimization for a list of Pareto-optimal solutions is shown in Figure 5. More specifically, Figure 5a shows that the district can become approximately carbon-neutral already for a relatively low overall investment cost (approx 12 CHF/$m^2$yr). This result is achieved also thanks to a significant contribution of energy generated from the PV panels installed on facades, which contribute to approximately 40% of the total PV surface installed, or 60% of the available facades area, corresponding to PV deployment on all the well-oriented facades.

Further increasing the allowed CAPEX only leads to a limited improvement in terms of total GWP of the solution, that caps at a total CAPEX of approximately 20 CHF/$m^2$yr. Beyond this limit, the overall GWP of the solution actually worsens: the increase in PV surface installed is compensated by the lower specific generation of PV panels installed on facades, and on the increasing battery capacity, which has little contribution to the overall energy balance, but increases costs and GWP potential.

The role of batteries is rooted in the tariffs imposed by the system operator, that are meant to favour solutions with reduced transmission peaks and improved self-sufficiency. As current tariffs (electricity cost = 20 ct/kWh and feed-in price = 8 ct/KWh) favor self-consuming locally generated energy over selling it to the grid, solutions with increased CAPEX bound tend to shift towards the increase of battery capacity as to reduce energy exchanges with the grid. This is shown clearly in Fig 5b: moving towards high-CAPEX solutions the imports at the district transformer decrease, together with exports: the energy locally generated increases only marginally, while the focus is shifted towards using it locally.

The reason behind the sharp increase in required storage size when the PV surface installed increases can be seen in Figure 6. At the low range, storage is only used for daily balancing purposes, thus requiring a very limited amount of storage size. In Figure 6, the first line appears basically flat, as the required daily storage is low.

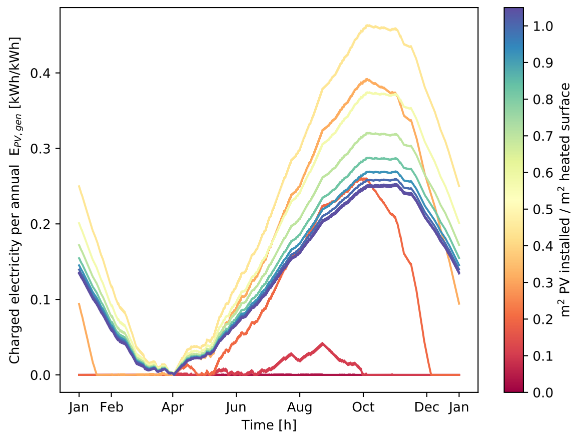


*Figure 6: State of charge of an storage system aiming at self sufficiency for different levels of PV penetration.*

At higher PV surfaces installed, achieving self sufficiency requires seasonal storage. All solutions where the ratio between PV installed surface and heated surface is above approximately 20% show a demand for seasonal storage. The state of charge of the storage peaks in the end of the summer, and then is gradually used during the winter.

The Table 4 summarize PV coverage needed for the implementation of future self-sufficient and carbon-neutral decentralized district energy system.

*Table 4: Solutions for future decentralized district*

| Solutions | PV coverage | | | |
|---|---|---|---|---|
| | $A_{PV}/A_{SRE}$ | roof | facade | total |
| full PV roof coverage, self-sufficiency 75% | 0.32 | 100.0% | 0.0% | 30.5% |
| **self-sufficiency, round-trip $\eta$=100%** | **0.44** | **100.0%** | **16.4%** | **41.9%** |
| self-sufficiency, round-trip$\eta$=85% | 0.53 | 100.0% | 28.8% | 50.5% |
| carbon-neutrality | 0.62 | 100.0% | 41.0% | 59.0% |
| self-sufficiency, round-trip $\eta$=59% | 0.81 | 100.0% | 67.1% | 77.1% |
| full PV coverage, self-sufficiency with $\eta$=50% | 1.05 | 100.0% | 100.0% | 100.0% |

## 7.2. Annual revenues

The results presented in Figure 5 represent Pareto-optimal solutions for the two competing objectives of minimizing OPEX and CAPEX. However, the choice of the individual prosumer will be influenced by the profitability of the investment, which is a result of the combined effects of CAPEX and OPEX. Policy makers and grid operators might be interested in knowing how different energy prices can influence the profitability of a PV investment, and hence the amount of PV installed and of resulting energy generated. From the prosumer perspective, this translates into the question ”how much PV panels can I install if I aim for the investment to pay back by the end of the PV panels’ lifetime?”; from the policymaker perspective, the question instead is ”how should tariffs be set in order to achieve the desired decentralized energy generation from PV panels?”.

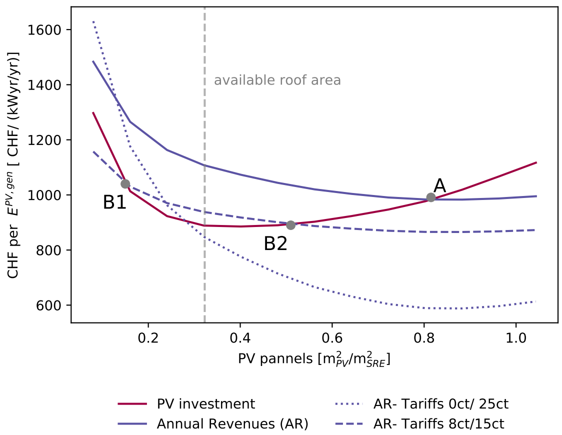


*(a)*

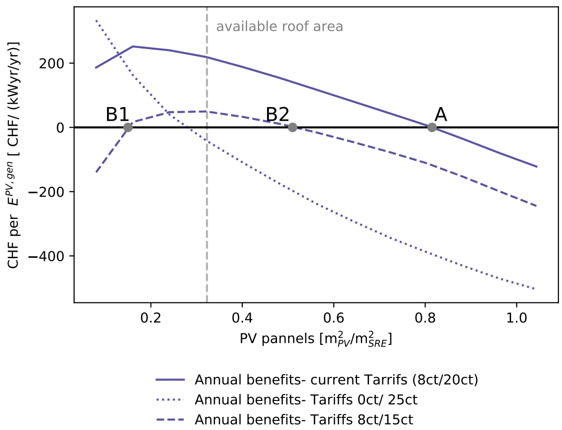


*(b)*

*Figure 7: a) PV investment per generated PV electricity $E^{PV,gen}$ and implicit revenues for different Feed-in/demand price. Economic point: Investment in PV and connected revenues are balanced. Point A - current Tariffs 8ct Feed in, 20 ct demand price; Points B1 and B2 exemplary Tariffs with two break even points. b) Annual benefits, which are the annual revenues subtracted by the PV investment.*

The extent to which facade solutions are cost efficient depends on installed surface is shown in Figure 7. The point A represents the surface of installed PV panels for which lifetime revenues and investment are equal. This shows that, with current tariffs, large surfaces of facades could be covered with PV panels, while still achieving a positive economic performance. This is strongly influenced by the choice of tariffs by the system operator.

At current tariffs (0.20 CHF/kWh for energy purchased from the grid, 0.08, CHF/kWh for energy sold to the grid) as mentioned before, large facade surfaces can be covered with PV panels in conditions where lifetime revenues are larger than the investment cost.

Lowering the purchase price (e.g., in this paper, the case with 0.15/0.08 CHF/kWh) tends to worsen the economic performance in the whole surface range, as it affects the portion of the generated solar energy that is self consumed. In this case, according to the optimization’s results, there is a limited window where PV is convenient: for installed surfaces below point B1 the fixed component of the investment is predominant. For installed surfaces higher than B2 the combination of two factors makes these solutions economically unfavourable: first, new PV panels are installed on surfaces that generate less energy per unit of surface installed. Second, every new panel will mostly contribute to the annual revenues with energy that is sold to the grid (and not self-consumed), which is paid less to the prosumer.

Finally, the effect of decreasing feed-in tariffs to 0 CHF/kWh is shown by the dotted line. In this case, facades should be discarded: only energy that is self consumed matter, so the most economically convenient choice is to install only few panels, only on roofs.

Evidently, the location of the ”zero-net performance point” depends on a combination of the two tariffs. This can be seen more clearly in Figure 8, where subfigure 8a shows the position of the point B1 (lowest installed surface that makes the installation of PV panels economically favourable). Moving towards the upper white area would substantially mean eliminating the entry barrier to new producers, especially smaller ones. This can be achieved by a combination of feed-in and purchase tariffs.

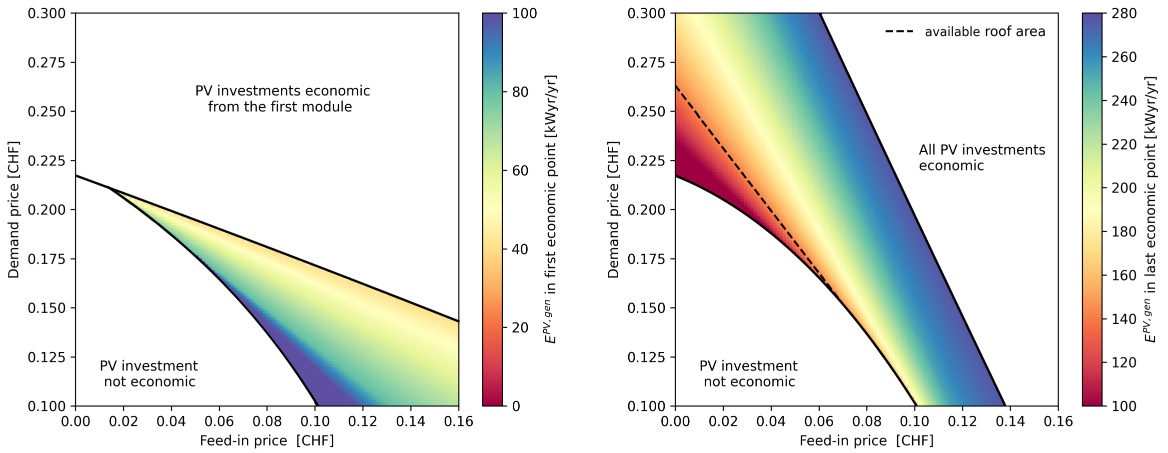


*(a)* *(b)*

*Figure 8: PV generation in break-even point for different Tariffs a) first break-even point (similar to B1) b) last econmic poit (B2 or A) in Figure 7*

It is however more interesting to look at the position of point B2 (highest economically favourable surface) in Figure 8b. This figure shows the importance of increasing feed-in prices if the objective is to maximize generation. For instance, even at today’s demand price, increasing the purchase price from 0.08 CHF/kWh to 0.10 CHF/kWh would theoretically make all roof and facade surfaces economically convenient.

## 7.3. PV distribution on roof and facade

The results of the optimization confirm what observed about the per-surface generation potential. The conclusions resulting from the analysis of these with respect to the potential from installing PV on facades are different depending on what side of the coin one looks at.

The general trend, as expected from what shown in Figure 4b, is that rooftop-PV has a much higher performance compared to facede-installed PV, which is clearly shown by the fact that panels are first installed on roofs. The comparison of Figure 9a and 9b shows clearly the reason: in ”high-CAPEX” solutions the PV investment cost for facades dominates the total investment, while it still provides less than half of the total energy generated.

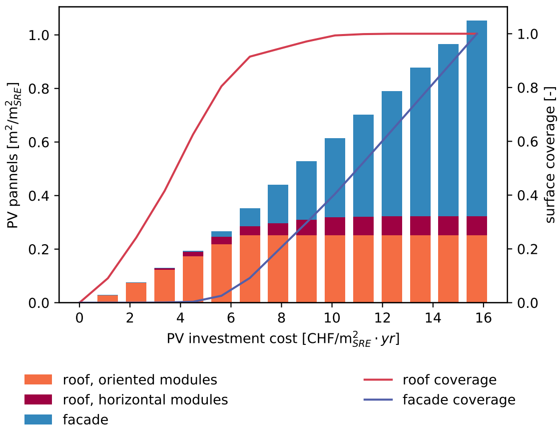


*(a)*

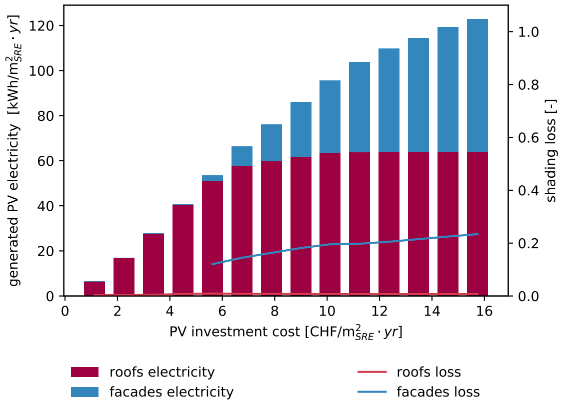


*(b)*

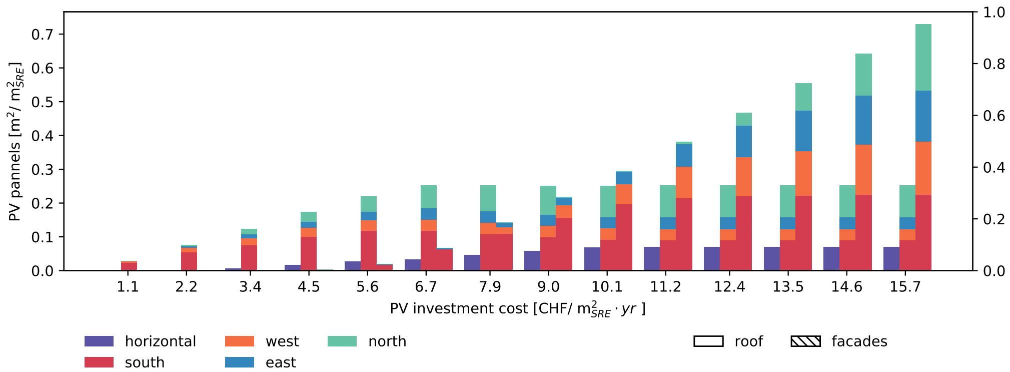


*(c)*

*Figure 9: Economically best PV installation for 44 residential buildings in a district with 70 buildings a) Area of installed modules sorted by orientation type, PV modules with tilt = 0°are horizontal, tilt angles = 90°are facades, oriented modules summarize all other tilt angles. b) Annual generated electricity and shading losses depending on surface type.*

However, looking at the same figures from another perspective, facades have the potential to increase the total energy generation from PV by approximately 80%. While they might not represent the most cost-efficient solution, they certainly can play an important role in improving the self-sufficiency of the district.

Looking more in detail at the surfaces where PV panels are installed depending on the optimization scenario, it can be noticed that some of the vertical surfaces are used even when roofs are not ”full” yet. This is a consequence of two factors: first, the fact that (as shown in Figure 4b some facades do have a higher specific PV generation potential than some roofs; second, the fact that the CAPEX-constraint is not enforced at district level, but at building level. This implies that when at district level there might still be 10% of roofs available, this might not be true at building level, where the optimizer is then ”forced” to start using facades instead. This same reasoning can also explain why the optimizer starts selecting East- and West-oriented facades even when thee are still South-oriented facades available.

## 7.4. Energy storage capacity

The results also show the extent of the variation. he average power generation from installed PV can range between 100 and 280 kW, showing that appropriately choosing electricity tariffs can lead to an increase of almost 200% of the yearly energy generated by PV panels in the district.

In previous results, it was shown that the district can achieve carbon neutrality relatively easily: this is true, however, when only balancing local energy generated with local energy demand. In truth, not all energy is used locally: part of it is sold to the grid, and purchased back in a second moment, thus using the grid as electrical storage. Depending on the efficiency that is assumed for the grid-as-storage, the amount of surface covered by panels increases.

If the storage is assumed to be lithium-ion batteries (which would be the most likely case for district-level storage, connected to the same low-voltage grid as the district), it is possible to assume a relatively high round-trip efficiency for the grid-as-storage. In Figure 10a the line for $\eta = 0.85$ can be used as reference, showing that in this case the PV surface need to be increased only marginally.

Another relevant point in Figure 10 is represented by the ”last economic point”, that is the largest amount of PV panels that can be installed with the expectation of recovering the investment within the panels’ lifetime with current tariffs. The efficiency of the grid-as-storage that allows self-sufficiency in this point is approximately 0.59. Incidentally, this is quite similar to the round-trip efficiency of pumped hydro storage (PHS), today the most common way of doing grid-level storage in Switzerland.

Finally, the case of $\eta = 40$% is shown, a relatively optimistic example of round-trip efficiency of power-to-gas storage systems. In this case, the results show that the available surface is simply not sufficient, and even covering all roofs and facades with PV panels would not allow to achieve self sufficiency of the district. The actual minimum efficiency that needs to be achieved by the selected combination of storage technologies to achieve self-sufficiency (that is, the efficiency that allows achieving self sufficiency when all surfaces in the district buildings are covered with PV panels) is $\eta = 50$%. Power-to-gas-to-power storage systems should aim at achieving at least this round-trip efficiency, if they should be used for grid storage purposes.

Figure 10b shows the perspective of the grid operator, when looking at the importance of the efficiency of the grid-as-storage. Grid revenues are obtained thanks to the difference between feed-in and purchase electricity prices, but also depend on the amount of energy that is lost in the irreversibilities of the storage charge/discharge process. The results show that the grid can, with the reference tariff assumed in this study, have positive income even with low storage efficiency. However, the grid also has a clear interest in working with high round-trip efficiency.

Interestingly, the installed PV surface that generates the maximum revenues changes depending on the grid efficiency: as the efficiency of the grid-as-storage decreases, the PV surface that generates the maximum revenues increases. This is because the peak is located where self-sufficiency for the system is achieved.

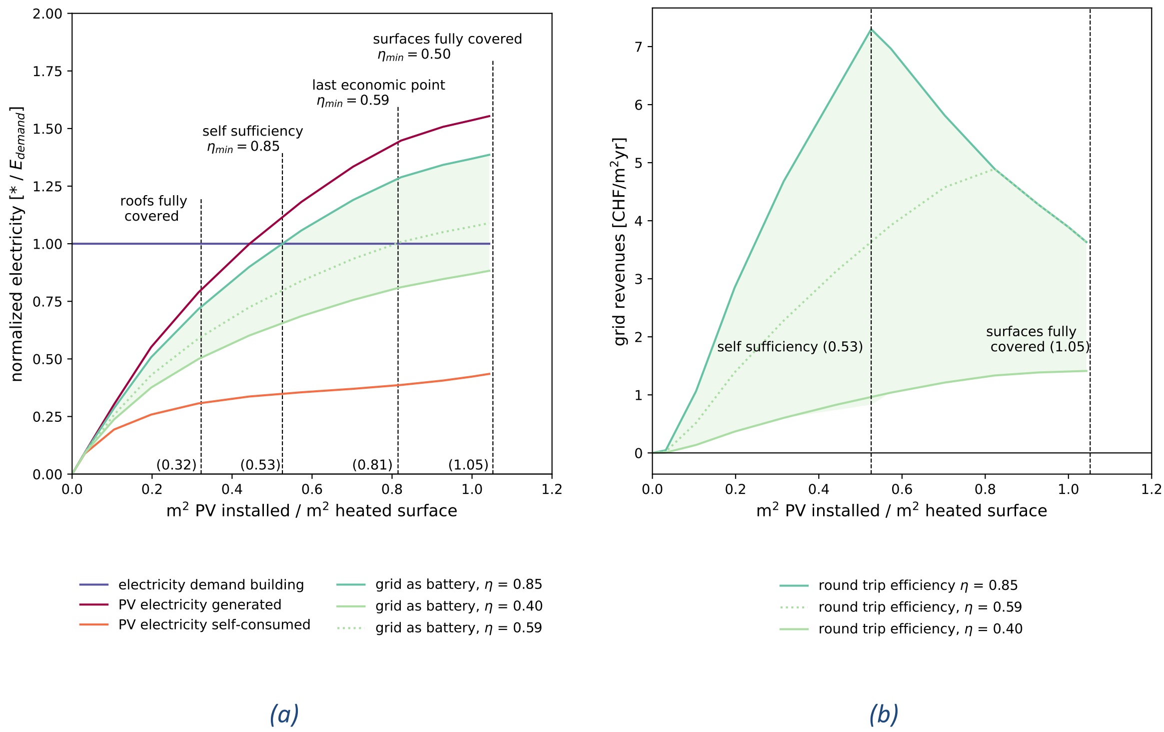


*Figure 10: a) The need of PV panels of 31 buildings balanced at the transformer to reach self-sufficiency with re-import. b) Revenues as a function of installed PV capacity and grid efficiency from the perspective of the grid. The grid buys electricity at a feed-in tariffs of 0.08 CHF/kWh and resells for electricity price 0.20 CHF/kWh*

The results shown in the previous sections highlighted that the district requires a relevant amount of storage in order to become self-sufficient. The actual amount of storage required is shown in Figure 11b, relative to the total amount of energy locally generated by PV panels. The results show that the storage capacity required in the case of ideal storage (100% round-trip efficiency) to achieve self-sufficiency is equal to more than 40% of the total amount of energy generated. The same results also show that the maximum storage time is larger than 8000 h.

The results shown so far focused on the application of one main technology to the district's energy system: PV panels. In addition, the study takes into account the fact that several local energy conversion technologies can be chosen (particularly for heating purposes). This is a reasonable choice, given that PV panels and efficient energy conversion technologies are among the most common solutions to choose among when dealing with energy efficiency in the built environment.

Building renovation is the most common other solution, which is favoured because it allows reducing the overall energy demand, rather than generating energy in a more sustainable way. While this is not the main focus of this study, it can definitely be interesting to answer to the question of how does the required storage capacity changes when the buildings' energy demand is reduced.

The results of this analysis are shown in Figure 11a. The results are shown for three main cases: reference

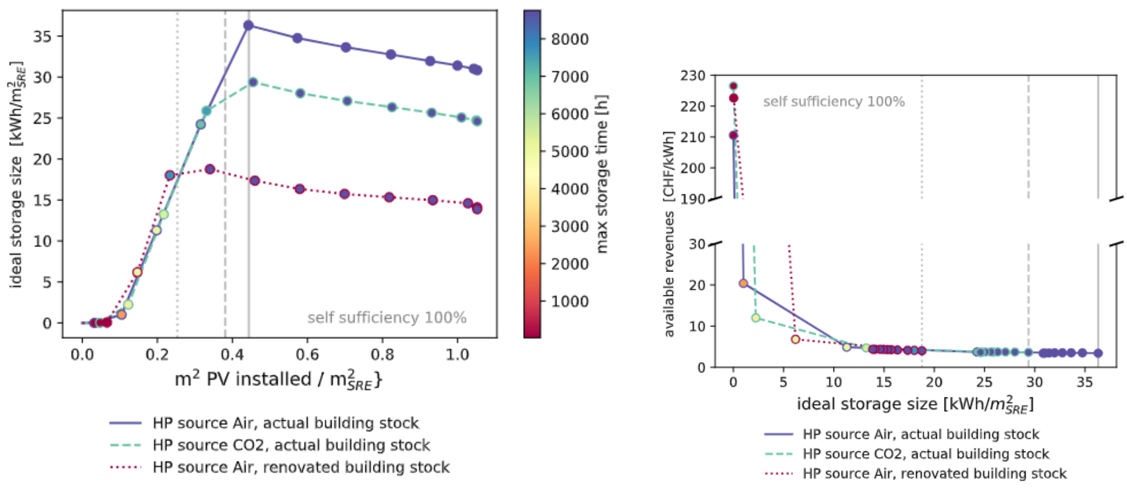


*(a)* *(b)*

*Figure 11: Key identifiers of an required storage system with round trip efficiency $\eta$= 100% to store surplus PV electricity for different efficiency strategies. a) required storage size and time b) directly available price form buying at feed in tariff of 0.08 CHF/kWh and selling at for electricity price 0.20 CHF/kWh*

case (air-source HP, actual building stock) referring to the results shown in the previous part of the paper; improved HP case, where high-efficiency Heat pump (HP)s using a $CO_2$ network as cold source (CIT); finally, renovated building stock case, with standard HPs but with isolated buildings.

The results show, as expected, that increasing the efficiency of the building stock, a very expensive measure, is the most efficient solution as it allows achieving self-sufficiency with a more limited amount of PV installed, a lower ideal size of the grid storage size, and lower maximum storage time. This result provides additional ground to the general trend of policies

Regardless of the type of retrofitting solution, can we afford this much storage in the system? While grid operators recur to a variety of means to store energy (from existing Pumped hydro storage (PHS) to simply balancing the grid with centralized power generation), it can be worth answering this question based on the idea that the grid operator is expected to only cover the expenses for purchasing the required storage capacity by using the revenues generated by the different demand/feed-in electricity prices.

The results of this analysis are shown in Figure 11b. Only the scenario with very limited PV panels installed generates enough revenues (compared to the amount of energy generated) to make it profitable from the perspective of the grid, assuming typical costs for lithium-ion energy storage. For all simulated cases apart from the one with the lowest PV surface installed, the amount of resources available for storage is below 20 CHF/kWh, with values ”converging” to about 5 CHF/kWh for storage sizes above 10 kW

The Table 5 summarize the reduction in storage capacity and PV coverage obtained through the renovation of the building stock and the implementation more efficient very low temperature 4G or 5G district heating network.

*Table 5: Impact on the PV covergage of building stock renovation and district heating implementation for self-sufficient district*

| Self-sufficiency solutions with round-trip $\eta$ = 100% | storage capacity | | PV covergage | |
|---|---|---|---|---|
| **Air HP** | **35.0** $kWh/m^2_{SRE}$ | | **41.9%** | |
| 4G/5G district heating network | 29.0 $kWh/m^2_{SRE}$ | -(17.1%) | 36.2% | -(13.6%) |
| Building envelope renovation | 18.8 $kWh/m^2_{SRE}$ | -(46.3%) | 23.8% | -(43.2%) |

# 8. Conclusions

This study aimed at investigating the potential of the implemented solution in residential district to increase their sustainability, even achieving climate neutrality and self-sufficiency, by using a combination of PV power generation, batteries, heat pumps and individual thermal storage.

The problem was addressed as a multi-objective, mixed integer-linear programming problem, with the OPEX and CAPEX of the system as competing objectives, and the installed sizes and operating load of the different energy conversion units (including PV panels and batteries) as optimization variables. Comparing to existing literature in the field, the proposed approach combines an advanced modelling of the energy generation potential from PV panels with a detailed representation of the district energy systems, down to the system of each individual building, thus allowing an accurate representation of the interaction between the energy generation from PV and the rest of the system.

The proposed approach was applied to a reference residential district of the RE demonstration site.

The results of the application of the proposed method to the case study allowed drawing the following conclusions:

**Facade PV specific energy potential** Facades have a high theoretical potential, based on their surface compared to roofs: the total facade surface in the district sums to about twice as much that of that of district rooftops. However, the worse angle with respect to solar radiation and the shading among buildings have the effect of significantly worsening their electricity generation potential. Overall, however, the installation of PV panels on facades has the potential of increasing the total energy generated by approximately 80%.

**PV placement order** The results of the multi-objective optimization show that, as excepted, PV panels are prioritized on roofs (first horizontal, then South-East-West-North) and only then on facades (South, East/West, North). This is clearly due to the higher specific energy generation potential of roofs compared to facades. The moment of the day when solar power is generated counts only to a lesser extent.

**Solar-driven district carbon neutrality** Facades can play an important role in the energy systems of districts. The results of the multi-objective optimization show that it is relatively cost efficient to achieve carbon neutrality, but that this is only possible if PV panels are also installed on facades, based on the current energy conversion units and building stock. Further additions of PV panels and batteries allow reducing operating costs but have little effect in further reducing the total GWP potential of the energy system.

**Economic convenience of facade PV** Facades are costly, and less cost-efficient compared to rooftop solar. However, the results of the analysis of the influence of electricity prices (both for purchasing electricity from the grid and feed-in) showed that there are many combinations of tariffs that make many (if not all) facades economically convenient over their lifetime. These results thus highlighted the important influence that electricity prices have on the maximum PV surface that can be covered while still being economically viable. Current tariffs would allow up to 80% of the total available surface to be covered.

**Achieving district self-sufficiency** Even if climate-neutrality can be achieved relatively easily, the same cannot be said for self sufficiency. This is because solar energy is not available at the times when it is needed, thus requiring feeding part of the energy to the grid, and purchasing it back at a different time. Depending on the assumption for the round-trip efficiency of the grid considered as a storage unit, it is more or less challenging to achieve self sufficiency for the district. This objective can be achieved by covering from approx. 40% to 100% of the available surface when the round trip efficiency decreases from 100% to 50%.

**Storage requirements** The results underlined the importance of storage for achieving self-sufficiency, and the fact that even when assuming a 100% round trip efficiency for the storage, very large storage capacities are required. The results also showed that the grid revenues generated by the difference between retail and feed-in prices are not sufficient to pay for the storage that is required to make the district self-sufficient, suggesting that public funding would be crucial for supporting these developments. This is true already at relatively low installed PV capacity ($A_{PV}/A_{SRE} = 0.2$), when storage starts to be required for seasonal instead of daily storage, thus increasing dramatically the required capacity and storage time.

**The role of building renovation** Of the solutions tested in this study, building renovation, with its important effect of energy demand reduction, was identified as the most promising in synergy with PV generation. This because building renovation allows reducing both the required installed PV and storage capacity to achieve self-sufficiency by half.

**The role of 5G district heating** The development of more efficient 4G or 5G district heating system will allow to reduce by more than 15% the size of the storage while reducing by about 15% the PV area. Moreover, the foreseen deployment of 5G district heating and cooling network is expected to realize sector coupling by introducing power to gas (P2G) and electro-thermal energy storage (ETES) capacity in the decentralized district energy system. .

# References


[1] Raluca Suciu, Luc Girardin, and François Maréchal. Energy integration of co2 networks and power to gas for emerging energy autonomous cities in europe. *Energy*, 157:830–842, 2018. https://www.sciencedirect.com/science/article/pii/S0360544218309034.

[2] Mathias Niffeler, Thomas Schluck, Curdin Derungs, Luc Girardin, Luise Middelhauve, and Lionel Bloch. Sccer ja-red - analysis of initial case and identification of potential use for renewables and waste heat at the building and district level - deliverable 1.1.1. *SCCER JA-RED Report*, page 22, 2019. http://infoscience.epfl.ch/record/268360.

[3] Lionel Bloch, Jordan Holweger, Nicolas Wyrsch, Hervé Tommasi, and Luc Girardin. Sccer ja-red - description of the multi-energy demonstration system in the re demo site - deliverable 1.2.1. *SCCER JA-RED Report*, page 25, 2017. http://infoscience.epfl.ch/record/268357.

[4] Lionel Bloch, Luc Girardin, Jordan Holweger, and Luise Middelhauve. 5d3 - a list of possible ancillary services for enhanced grid operation and implementation of the most effective ones at the re demo site., page 45, 2020.

[5] Paul Stadler, Luc Girardin, Araz Ashouri, and François Maréchal. Contribution of Model Predictive Control in the Integration of Renewable Energy Sources within the Built Environment. *Frontiers in Energy Research*, 6, May 2018. http://journal.frontiersin.org/article/10.3389/fenrg.2018.00022/full.

[6] Raphael Wu, Georgios Mavromatidis, Kristina Orehounig, and Jan Carmeliet. Multiobjective optimisation of energy systems and building envelope retrofit in a residential community. *Applied Energy*, 190:634–649, March 2017. https://linkinghub.elsevier.com/retrieve/pii/S0306261916319419.

[7] John A. Duffie and William A. Beckman. *Solar engineering of thermal processes / John A. Duffie, William A. Beckman*. John Wiley, Hoboken, 4th ed edition, 2013.

[8] Luise Middelhauve, Francesco Baldi, Paul Stadler, and François Maréchal. Grid-Aware Layout of Photovoltaic Panels in Sustainable Building Energy Systems. *Frontiers in Energy Research*, 8:573290, February 2021. https://www.frontiersin.org/articles/10.3389/fenrg.2020.573290/full.

[9] Samuel Henchoz, Céline Weber, François Maréchal, and Daniel Favrat. Performance and profitability perspectives of a CO2 based district energy network in Geneva's City Centre. *Energy*, 85:221–235, June 2015. https://linkinghub.elsevier.com/retrieve/pii/S0360544215003886.

[10] Oswaldo Lucon and et. al. Buildings. In *Climate Change 2014: Mitigation of Climate Change. Contribution of Working Group III to the Fifth Assessment Report of the Intergovernmental Panel on Climate Change*. Cambridge University Press, United Kingdom and New York, 2014.

[11] Tillmann Lang, Erik Gloerfeld, and Bastien Girod. Dont just follow the sun – A global assessment of economic performance for residential building photovoltaics. *Renewable and Sustainable Energy Reviews*, 42:932–951, February 2015. https://linkinghub.elsevier.com/retrieve/pii/S1364032114009022.

[12] Dorota A. Chwieduk. Recommendation on modelling of solar energy incident on a building envelope. *Renewable Energy*, 34(3):736–741, March 2009. https://linkinghub.elsevier.com/retrieve/pii/S0960148108001766.

[13] S. Freitas, C. Reinhart, and M.C. Brito. Minimizing storage needs for large scale photovoltaics in the urban environment. *Solar Energy*, 159:375–389, 2018. https://www.scopus.com/inward/record.uri?eid=2-s2.0-85033494631&doi=10.1016%2fj.solener.2017.11.011&partnerID=40&md5=19fdd3b1cbad6754004886538f4275bc.

[14] P. Redweik, C. Catita, and M. Brito. Solar energy potential on roofs and facades in an urban landscape. *Solar Energy*, 97:332–341, November 2013. https://linkinghub.elsevier.com/retrieve/pii/S0038092X13003460.

[15] C. Catita, P. Redweik, J. Pereira, and M.C. Brito. Extending solar potential analysis in buildings to vertical facades. *Computers and Geosciences*, 66:1–12, 2014. https://www.scopus.com/inward/record.uri?eid=2-s2.0-84894264980&doi=10.1016%2fj.cageo.2014.01.002&partnerID=40&md5=784b366b487d59fc375840d745fcdfad.

[16] Emmanuel Walter and Jérôme Henri Kämpf. A verification of citysim results using the bestest and monitored consumption values. *Proceedings of the 2nd Building Simulation Applications conference*, pages 215–222, 2015. http://infoscience.epfl.ch/record/214754.

[17] A. Verso, A. Martin, J. Amador, and J. Dominguez. GIS-based method to evaluate the photovoltaic potential in the urban environments: The particular case of Miraflores de la Sierra. *Solar Energy*, 117:236–245, July 2015. https://linkinghub.elsevier.com/retrieve/pii/S0038092X15002066.

[18] G. Desthieux, C. Carneiro, R. Camponovo, P. Ineichen, E. Morello, A. Boulmier, N. Abdennadher, S. Dervey, and C. Ellert. Solar energy potential assessment on rooftops and facades in large built environments based on lidar data, image processing, and cloud computing. Methodological background, application, and validation in geneva (solar cadaster). *Frontiers in Built Environment*, 4, 2018. https://www.scopus.com/inward/record.uri?eid=2-s2.0-85061601695&doi=10.3389%2ffbuil.2018.00014&partnerID=40&md5=b2a7ad9c0270b8da2ab2e5fea8c2b7bf.

[19] Jérôme Henri Kämpf, Marylène Montavon, Josep Bunyesc, Raffaele Bolliger, and Darren Robinson. Optimisation of buildings' solar irradiation availability. *Solar Energy*, 84(4):596–603, 2010. https://www.sciencedirect.com/science/article/pii/S0038092X09001819.

[20] M.C. Brito, S. Freitas, S. Guimarães, C. Catita, and P. Redweik. The importance of facades for the solar PV potential of a Mediterranean city using LiDAR data. *Renewable Energy*, 111:85–94, October 2017. https://linkinghub.elsevier.com/retrieve/pii/S0960148117302768.

[21] C. Chatzipoulka, R. Compagnon, J. Kaempf, and M. Nikolopoulou. Sky view factor as predictor of solar availability on building façades. *Solar Energy*, 170:1026–1038, 2018. https://www.scopus.com/inward/record.uri?eid=2-s2.0-85048817338&doi=10.1016%2fj.solener.2018.06.028&partnerID=40&md5=f6df5c19e5d83bc97e77edaed07e7dc8.

[22] Naveed Rehman, Timothy Anderson, and Roy Nates. Diffuse Solar Potential of Facades in an Urban Context under Different Sky Conditions. *Asia-Pacific Solar Research Conference*, December 2018.

[23] S. Aguacil, S. Lufkin, and E. Rey. Active surfaces selection method for building-integrated photovoltaics (BIPV) in renovation projects based on self-consumption and self-sufficiency. *Energy and Buildings*, 193:15–28, 2019. https://www.scopus.com/inward/record.uri?eid=2-s2.0-85063346625&doi=10.1016%2fj.enbuild.2019.03.035&partnerID=40&md5=822191b4fd5026f87e72a3fa73a5c1bd.

[24] Y. Li and C. Liu. Techno-economic analysis for constructing solar photovoltaic projects on building envelopes. *Building and Environment*, 127:37–46, 2018. https://www.scopus.com/inward/record.uri?eid=2-s2.0-85033605717&doi=10.1016%2fj.buildenv.2017.10.014&partnerID=40&md5=0cfd8e17913603df2687bee398a8eeb6.

[25] M. Díez-Mediavilla, M.C. Rodríguez-Amigo, M.I. Dieste-Velasco, T. García-Calderón, and C. Alonso-Tristán. The PV potential of vertical façades: A classic approach using experimental data from Burgos, Spain. *Solar Energy*, 177:192–199, 2019. https://www.scopus.com/inward/record.uri?eid=2-s2.0-85056586994&doi=10.1016%2fj.solener.2018.11.021&partnerID=40&md5=319c7e2bc6e84b176683e184a359f119.

[26] S. Horn, E. Bagda, K. Brandau, and B. Weller. Influence of building-integrated photovoltaics in façades for the energetic evaluation of buildings. Part 1: Potential of façade integration of photovoltaics. *Bauphysik*, 40(2):68–73, 2018. https://www.scopus.com/inward/record.uri?eid=2-s2.0-85045429253&doi=10.1002%2fbapi.201810007&partnerID=40&md5=c1241cb9acfabea8ffa6ff71e26d6198.

[27] L.S. Pantić, T.M. Pavlović, D.D. Milosavljević, D.L. Mirjanić, I.S. Radonjić, and M.K. Radović. Electrical energy generation with differently oriented photovoltaic modules as façade elements. *Thermal Science*, 20(4):1377–1386, 2016. https://www.scopus.com/inward/record.uri?eid=2-s2.0-84991666493&doi=10.2298%2fTSCI150123157P&partnerID=40&md5=184eab99c7c46990c3de855858b49131.

[28] Paul Michael Stadler. *Model-based sizing of building energy systems with renewable sources*. PhD thesis, EPFL, 2019. http://infoscience.epfl.ch/record/267499/files/EPFL_TH9560.pdf.

[29] Richard Turton, editor. *Analysis, synthesis, and design of chemical processes*. Prentice Hall, Upper Saddle River, NJ, 4th ed edition, 2012.

[30] Rasmus Luthander, Joakim Widén, Daniel Nilsson, and Jenny Palm. Photovoltaic self-consumption in buildings: A review. *Applied Energy*, 142:80–94, March 2015. https://linkinghub.elsevier.com/retrieve/pii/S0306261914012859.

[31] Kantor Ivan and Alessio Santecchia. D5.7 – Report on LC assessment tools based on the results of MORE and EPOS. *Coordinated Production For Better Resource Efficiency*, May 2019. www.copro-project.eu.

[32] Gregor Wernet, Christian Bauer, Bernhard Steubing, Jürgen Reinhard, Emilia Moreno-Ruiz, and Bo Weidema. The ecoinvent database version 3 (part I): overview and methodology. *The International Journal of Life Cycle Assessment*, 21(9):1218–1230, September 2016. http://link.springer.com/10.1007/s11367-016-1087-8.

[33] Dimitrios-Sotirios Kourkoumpas, Georgios Benekos, Nikolaos Nikolopoulos, Sotirios Karellas, Panagiotis Grammelis, and Emmanouel Kakaras. A review of key environmental and energy performance indicators for the case of renewable energy systems when integrated with storage solutions. *Applied Energy*, 231:380–398, December 2018. https://linkinghub.elsevier.com/retrieve/pii/S0306261918313527.

[34] SIA. 2024:2025 Raumnutzungsdaten für die Energie- und Gebäudetechnik. *Schweizerischer Ingenieur und Architektenverein*, 2015.

[35] SIA. SIA 385/2:2015 Anlagen für Trinkwarmwasser in Gebäuden - Warmwasserbedarf, Gesamtanforderungen und Auslegung. *Schweizerischer Ingenieur und Architektenverein*, 2015.

[36] Jordan Holweger, Marina Dorokhova, Lionel Bloch, Christophe Ballif, and Nicolas Wyrsch. Unsupervised algorithm for disaggregating low-sampling-rate electricity consumption of households. *Sustainable Energy, Grids and Networks*, 19:100244, September 2019. https://linkinghub.elsevier.com/retrieve/pii/S2352467719300748.

[37] R. Perez, R. Stewart, C. Arbogast, R. Seals, and J. Scott. An anisotropic hourly diffuse radiation model for sloping surfaces: Description, performance validation, site dependency evaluation. *Solar Energy*, 36(6):481–497, 1986. https://linkinghub.elsevier.com/retrieve/pii/0038092X86900137.

[38] R. Perez, R. Seals, and J. Michalsky. All-weather model for sky luminance distribution—Preliminary configuration and validation. *Solar Energy*, 50(3):235–245, March 1993. http://www.sciencedirect.com/science/article/pii/0038092X9390017I.

[39] Darren Robinson and Andrew Stone. Irradiation modelling made simple: the cumulative sky approach and its applications. *Plea2004 - The 21st Conference on Passive and Low Energy Architecture*, January 2004.

[40] Mostapha Sadeghipour Roudsari and Adrian Adrian Smith Gordon Gill Architecture. Ladybug: A parametric environmental plugin for grasshopper to help designers create an environmentally-conscious design. In *Proceedings of BS2013*, Chambéry France, August 2013. https://www.researchgate.net/publication/287778694_Ladybug_A_parametric_environmental_plugin_for_grasshopper_to_help_designers_create_an_environmentally-conscious_design.

[41] Federal Statistical Office. Federal register of buildings and dwellings (rbd), 2019. https://www.bfs.admin.ch/bfs/en/home/registers/federal-register-buildings-dwellings.html.

[42] Federal Office of Topography swisstopo. swissbuildings3d 2.0 - 3d building models of switzerland, 2019. https://s.geo.admin.ch/8f6be8b96d.

[43] Federal Office of Meteorology and Climatology MeteoSwiss. Solar potential of all roofs and facades in switzerland, 2019. https://www.uvek-gis.admin.ch/BFE/sonnendach/?lang=en.

[44] SIA. SIA 380/1:2016 Heizwärmebedarf. *Schweizerischer Ingenieur und Architektenverein*, 2016.

[45] Luc Girardin. *A GIS-based Methodology for the Evaluation of Integrated Energy Systems in Urban Area*. PhD thesis, EPFL, 2012. http://infoscience.epfl.ch/record/170535/files/EPFL_TH5287.pdf.

[46] J. Remund, S. Kunz, METEOTEST, and METEOTEST Swiss Federal Office of Energy. Meteonorm - global meteorological database for engineers, planners and education, 2003.

[47] DOE. Weather Data | EnergyPlus, U.S. Department of Energy's (DOE) Building Technologies Office (BTO) and National Renewable Energy Laboratory (NREL)., March 2020. https://energyplus.net/weather.

[48] Administration cantonale vaudoise. Géodonnées etat de vaud , cadastre des bâtiments, 2019. https://www.geo.vd.ch/?center=2516088,1146375&scale=3780&wkid=2056&theme=asitvd_couleur&mapresources=GEOVD_MENSURATION&visiblelayers={"GEOVD_MENSURATION":["Bâtiments","Bâtimentsprojetés","Couverts:mens.officielle","Couverts:saisieprovisoire","N°debâtiments"]}.

[49] OpenStreetMap contributors. Planet dump retrieved from https://planet.osm.org , 2017. https://www.openstreetmap.org.

[50] Administration cantonale vaudoise. Géodonnées etat de vaud , registre cantonal des bâtiments (rcb), 2019. https://www.geo.vd.ch/?center=2516088,1146375&scale=3780&wkid=2056&theme=asitvd_couleur&mapresources=GEOVD_MENSURATION&visiblelayers={"GEOVD_MENSURATION":["Bâtiments","Bâtimentsprojetés","Couverts:mens.officielle","Couverts:saisieprovisoire","N°debâtiments"]}.

[51] Swiss Federal Office of Energy - Geoinformation - Sonnendach.ch. 3d data of roof area by the swiss federal office of topography swisstopo, 2018. https://github.com/SFOE/sonnendach-ui.

[52] Romande Energie SA. Distribution networks database, 2018. www.romande-energie.ch.

[53] Daniel Klauser. Solarpotentialanalyse für Sonnendach.ch Schlussbericht. Technical report, Bundesamt für Energie BFE, Bern, February 2016.